KTH Engineering Sciences

Master Thesis

Yet Another Thesis About Diagrammatic Monte Carlo

Emil Blomquist

Theoretical Particle Physics, Department of Physics,
School of Engineering Sciences
Royal Institute of Technology, SE-106 91 Stockholm, Sweden

Stockholm, Sweden 2017

Typeset in LaTeX

TRITA-???
ISSN ???
ISRN ???

Printed in Sweden by Universitetsservice US AB, Stockholm September 2017

Abstract

...

Sammanfattning

...

Preface

...

Contents

Comments guide

- Something about an image
- Motivation for myself
- Question about something
- There is something wrong, a flaw
- Todo, things which need to be done at some point

Notations

Units

Throughout this text $k_B = \hbar = 1$ has been used. With this notation there no difference between wave vectors and momentum.

Fourier transform

A function $f(x)$ which is defined and integrable on the interval $x \in [-L/2, L/2]$ may be represented as a Fourier series. In this thesis the following convention will be used

$$c_k \equiv \int_{-L/2}^{L/2} f(x)\, e^{-ik\cdot x}\, \mathrm{d}x \quad \Rightarrow \quad f(x) = \frac{1}{L}\sum_k c_k\, e^{ik\cdot x}\,. \tag{1}$$

where the wave vectors are given by $k = 2\pi n/L$ and $n \in \mathbb{Z}$. In the limit $L \to \infty$ the Fourier transform is defined accordingly

$$\hat{f}(k) \equiv \int_{\mathbb{R}} f(x)\, e^{-ik\cdot x}\, \mathrm{d}x \quad \Rightarrow \quad f(x) = \frac{1}{2\pi}\int_{\mathbb{R}} \hat{f}(k)\, e^{ik\cdot x}\, \mathrm{d}k\,. \tag{2}$$

How does this definition affect the conjugate variables in the derivation of the Fröhlich Hamiltonian?

Perhaps mention something about DOS and motivate

$$\frac{1}{V}\sum_{\mathbf{k}} \cdots \to \int \frac{\mathrm{d}^3k}{(2\pi)^3} \cdots\,. \tag{3}$$

TODO's

- Up in the corner: Contents → Notations
- Rewrite the text so the word *we* is nowhere to be found
- Use either $\mathbf{x}$ or $\mathbf{r}$
- In the finite temperature formalism: expectation value → ensemble average
- Sometime: momentum → wave vector
- Perhaps use "in spite"
- "as well as" ↔ "along with"
- set proper size of the figures in the DMC examples

- $\mathcal{G}_0, \mathcal{D}_0 \rightarrow \mathcal{G}^{(0)}, \mathcal{D}^{(0)}$. Make sure that this does not affect the zeroth order bold-line $\mathcal{G}_0$!
- Remove Feynman diagram helping backgrounds

Chapter 1

Introduction

- Quantum mechanics
- Many-particle physics
- References to recent articles about polarons and DMC
- mention something out of the polaron book?

Chapter 2

Background material

Here we shall summarize what this chapter is about

2.1 Quantum field theories

2.1.1 Single- and many-particle quantum mechanics

In quantum mechanics, utilizing the bra-ket notation, the state of a particle $|\psi\rangle$ can be projected onto the position basis $|\mathbf{x}\rangle$ to form a wave function $\langle\mathbf{x}|\psi\rangle = \psi(\mathbf{x})$. By using the Schrödinger picture, the dynamics is also contained within the states, i.e. $|\psi\rangle = |\psi(t)\rangle$ and $\psi(\mathbf{x}) = \psi(\mathbf{x}, t)$. Thus, assuming there is no external potential acting on this particle, the time evolution in terms of the wave vector is in the non-relativistic case governed by the Schrödinger equation. The quantity $\psi^*(\mathbf{x}, t)\psi(\mathbf{x}, t)$ is real, and according to the Copenhagen interpretation of quantum mechanics it is to be interpreted as the probability density function[citation]. The complex conjugated wave function is obtained by $\psi^*(\mathbf{x}, t) = (\langle\mathbf{x}|\psi(t)\rangle)^* = \langle\psi(t)|\mathbf{x}\rangle$. From this, the expectation value of some quantity, e.g. the position of the particle, is acquired through

$$\begin{aligned}
\langle\mathbf{x}(t)\rangle &= \int \psi^*(\mathbf{x}, t)\psi(\mathbf{x}, t)\,\mathrm{d}^3x \\
&= \int \mathbf{x}\,\langle\psi(t)|\mathbf{x}\rangle\langle\mathbf{x}|\psi(t)\rangle\,\mathrm{d}^3x \\
&= \langle\psi(t)|\left[\int \mathbf{x}\,|\mathbf{x}\rangle\langle\mathbf{x}|\,\mathrm{d}^3x\right]|\psi(t)\rangle \\
&= \langle\psi(t)|\,\hat{\mathbf{x}}\left[\int |\mathbf{x}\rangle\langle\mathbf{x}|\,\mathrm{d}^3x\right]|\psi(t)\rangle \\
&= \langle\psi(t)|\,\hat{\mathbf{x}}\,|\psi(t)\rangle\,.
\end{aligned} \tag{2.1}$$

That is, sandwich the operator of the sought observable in between the corresponding bra and ket of the particle state. Used to reach the final equality is that the position basis is an eigenbasis of the position operator $\hat{\mathbf{x}}|\mathbf{x}\rangle = \mathbf{x}|\mathbf{x}\rangle$ and the fact that this basis is orthonormal so that the unity operator might be expressed as $\hat{\mathbb{1}} = \sum_{\mathbf{x}} |\mathbf{x}\rangle\langle\mathbf{x}|$.

- Mention Hilbert space. one particle vs. many-particle Hilbert spaces.
- Perhaps quickly mention the Heisenberg picture here?

What has been described so far is single-particle quantum mechanics. However, it is possible to generalize this formalism to many-particle quantum mechanics. In the simple case of N distinguishable particles, the state of the system will be described by

talk only about indistinguishable particles

$$\begin{aligned} |\psi(t)\rangle &= |\psi_0(t)\rangle \otimes |\psi_1(t)\rangle \otimes \cdots \otimes |\psi_{N-1}(t)\rangle \\ &= |\psi_0(t),\, \psi_1(t),\, \ldots,\, \psi_{N-1}(t)\rangle\,, \end{aligned} \tag{2.2}$$

where the $|\psi_i(t)\rangle$'s are single-particle states multiplied together by tensor products. For indistinguishable particles things become more complicated due to statistics. That is, the state of the entire system must be symmetric when a pair of bosonic single-particle states are exchanged, and similarly for fermions it must be antisymmetric. Another shortcoming with this description of quantum mechanics is that the number of particles of each species must be fixed. Hence it is not possible to have particle creation nor particle annihilation, which is necessary for certain processes.

2.1.2 Second-quantization

The second quantization is a Hamiltonian based method for constructing a quantum field theory. Such a theory does not have the shortcomings of having a fixed set of particles as in the case of the many-particle description of quantum mechanics.

Again the state of the total system will be described by individual single-particle states. However, instead of having explicit all the permutations of the indistinguishable single-particle states, we will now express the total system state using occupation numbers. That is, in this representation the only information given is for each species of particle, the number of particles occupying what states. For example, given the following set of single-particle states $\{|\nu_i\rangle\}$ where $i = 0,\, 1,\, 2,\, \ldots$, the expression describing a state in which $|\nu_0\rangle$ and $|\nu_2\rangle$ is occupied by three and two particles respectively would then be $|3,\, 0,\, 0,\, 2,\, 0,\, 0,\, \ldots\rangle$.

In order to allow for the number of particles to be variable the Fock space is used. This space is a combination of Hilbert state spaces for any number of particles; from the empty vacuum state to a state with infinite particles. In order to create and

annihilate a particle of a certain quantum number, creation $\hat{c}_\nu^\dagger$ and annihilation $\hat{c}_\nu$ operators are used. It can be shown that they are the Hermitian conjugate of one another which motivates the notation. These operators incorporate the underlaying statistics of the particle at hand by a set of commutation relations. For bosons they are

$$[\hat{a}_i, \hat{a}_j^\dagger] = \delta_{ij} \,, \quad [\hat{a}_i, \hat{a}_j] = [\hat{a}_i^\dagger, \hat{a}_j^\dagger] = 0 \,. \tag{2.3}$$

These commutation relations are, for each single-particle state, identical to the ladder operators of a harmonic oscillator. For fermions the commutation relations are identical, but the commutator is exchanged in favor of the anticommutator in order to make the state antisymmetric,

$$\{\hat{b}_i, \hat{b}_j^\dagger\} = \delta_{ij} \,, \quad \{\hat{b}_i, \hat{b}_j\} = \{\hat{b}_i^\dagger, \hat{b}_j^\dagger\} = 0 \,. \tag{2.4}$$

One interesting property arise from the relation $\{\hat{b}_i^\dagger, \hat{b}_i^\dagger\} = \hat{b}_i^\dagger \hat{b}_i^\dagger + \hat{b}_i^\dagger \hat{b}_i^\dagger = 0$, the implication of which become apparent when trying to create two or more particles sharing the same single-particle state; a zero will be multiplied by the resulting state. Hence all observables computed using such a state will be exactly zero. This would affect the physics equally to there being no state of this sort which of course is nothing but the Pauli exclusion principle.

2.1.3 Field operators

When having utilized the second-quantization formalism, the quantum mechanical system is described by a quantum field. That is, rather than being an operator as in single- and many-particle quantum mechanics, the position is now a parameter, just like the time.

Field operators are creation and annihilation operators just like any other. They have gained their special name simply because they change the occupation number of single-particle eigenstates of the position operator. That is, they create nor annihilate at a particular position in space. (rephrase this shit!)

Using wave functions $\psi_\nu(\mathbf{x})$ corresponding to a complete orthonormal set of single-particle states $|\nu\rangle$ along with the creation and annihilation operator $\hat{c}_\nu^\dagger$, $\hat{c}_\nu$, the field operators may be constructed by the following superposition[1],

$$\hat{\psi}(\mathbf{x}) \equiv \sum_\nu \hat{c}_\nu \psi_\nu(\mathbf{x}) \,, \quad \hat{\psi}^\dagger(\mathbf{x}) \equiv \sum_\nu \hat{c}_\nu \psi_\nu(\mathbf{x}) \,. \tag{2.5}$$

The $\hat{\psi}(\mathbf{x})$ will annihilate a particle at position $\mathbf{x}$ whilst $\hat{\psi}^\dagger(\mathbf{x})$ will do the opposite and create a particle at position $\mathbf{x}$.

show special case of the quantum numbers $\{\nu\}$ being momentum.

2.2 A few words about finite temperature formalism

Point out that we are summarizing from Fetter Walecka.

When working with field theories at $T = 0$, even if the ground state is not the vacuum one, one does not need to be concerned about thermodynamics. At $T \neq 0$ however, unless the ground state is the vacuum, things are different. Although the formalism at finite temperature is interesting in itself, and much time could be spent discussing it, will only mention some similarities and differences relative the $T = 0$ formalism. Perhaps we will not even cover that, but only the absolute basics

Treating a system with variable number of particles at finite temperature, it is beneficial to work with the grand canonical ensemble. The partition function is then given by $Z_{\mathrm{G}} = \mathrm{Tr}\, e^{-\beta(\hat{H}-\mu\hat{N})} = \mathrm{Tr}\, e^{-\beta\hat{K}}$. Here β is the inverse temperature (recall that we use units where $k_{\mathrm{B}} = 1$), $\hat{H}$ is the Hamiltonian, $\hat{N}$ is the number operator, μ is the chemical potential and the trace is taken over a complete set of states. Introduced was also the grand canonical Hamiltonian $\hat{K} \equiv \hat{H} - \mu\hat{N}$. In accordance to the partition function, the statistical operator is then defined as $\hat{\rho}_{\mathrm{G}} = e^{-\beta\hat{K}}/Z_{\mathrm{G}}$.

At zero temperature the Heisenberg picture was used when calculating observables. In this picture the operators are responsible for the time evolution of the observables whilst the state vectors are made time independent. Moreover, an operator in the Heisenberg picture is related to the corresponding operator in the Schrödinger picture through $\hat{O}_{\mathrm{H}}(t) \equiv e^{i\hat{H}t}\,\hat{O}_{\mathrm{S}}\,e^{-i\hat{H}t}$. To calculate an observable from an operator, one would at $T = 0$ simply sandwiches the operator in between the ground state vector as such, $O(t) = \langle\Psi_0|\hat{O}_{\mathrm{H}}(t)|\Psi_0\rangle$. At finite temperature however, the observable is not given by merely an expectation value from a single state. As pointed out before, the statistics need now to be woven in. In accordance with the partition function, the observable should instead be sandwiched in between a complete set of states, and each weighted using the statistical operator,

$$O(t) = \sum_{\nu}\langle\Psi_\nu|\hat{\rho}_{\mathrm{G}}\,\hat{O}_{\mathrm{H}}(t)|\Psi_\nu\rangle \equiv \mathrm{Tr}\{\hat{\rho}_{\mathrm{G}}\,\hat{O}_{\mathrm{H}}(t)\}\,. \tag{2.6}$$

In equation (2.6) above, we have both real and imaginary exponents coming from the thermodynamics and quantum mechanics respectively (is it correct to say that, or do I need to be more specific?). In order to proceed, it would be convenient if one could treat the two types of exponents on an equal footing, and in order to do so a new picture is introduced. This is a modified Heisenberg picture where a Wick rotation in time $\tau = it$ is preformed, and the Hamiltonian is exchanged in favor of the grand canonical Hamiltonian. An operator in this picture is then related to itself in the Schrödinger picture as $\hat{O}_{\mathrm{K}}(\tau) \equiv e^{\hat{K}\tau}\,\hat{O}_{\mathrm{S}}\,e^{-\hat{K}\tau}$.

From this a perturbative treatment of an expectation value can be developed in a similar manner to what is done at zero temperature.

Insert equation of an observable expressed as a perturbation series. (2.7)

Should I write about having to do an analytical continuation of the temperature greens function in order to obtain frequencies and lifetimes of the excited states at finite temperature? Since we are not concerned about that in this thesis I recon that would be a waste of time.

2.2.1 Green's function

Introduce also the synonymous word *propagator*.

The Green's function, playing an important role when analyzing an interacting many-particle system, is the quantity of greatest interest in this thesis. At zero temperature, in position and time representation, the single-particle Green's function is defined as

$$iG_{\alpha\beta}(x,x') \equiv \frac{\langle\Psi_0|T[\hat{\psi}_{\mathrm{H}\alpha}(x)\hat{\psi}^{\dagger}_{\mathrm{H}\beta}(x')]|\Psi_0\rangle}{\langle\Psi_0|\Psi_0\rangle}\,. \tag{2.8}$$

Here $|\Psi_0\rangle$ is the ground state vector in the Heisenberg picture, $\hat{\psi}_{\mathrm{H}\alpha}(x)$ is the α-th component of a field operator also in the Heisenberg picture, $T[\cdots]$ orders the operators according to their time and x, x' being position-time four vectors.

Discuss the interpretation of a Green's function: G^2 is the probability of finding a particle at x which was introduced into the system at x'.

This Green's function contains observable properties such as both the ground state energy and the excitation spectrum of the system. By using the Lehman representation, the expectation value of any single-particle operator in the ground state of the system might also be extracted [1].

Above zero temperature, now working with an imaginary-time τ, the Green's function of interest to us is the temperature Green's function. In the imaginary-time and position representation, the corresponding single-particle temperature Green's function is defined through

$$\mathcal{G}_{\alpha\beta}(x,x') \equiv \mathrm{Tr}\{\hat{\rho}_{\mathrm{G}}\, T_{\tau}[\hat{\psi}_{\mathrm{K}\alpha}(x)\hat{\psi}^{\dagger}_{\mathrm{K}\alpha}(x')]\}\,. \tag{2.9}$$

What about the sign!? According to wikipedia the sign should not be there. The sign is chosen differently compared to Fetter Walecka.

Here $\psi_{\mathrm{K}\alpha}(x)$ is the α-th component of a field operator in the modified Heisenberg picture, $T_{\tau}[\cdots]$ orders the operators according to their value of τ, $\mathrm{Tr}\{\rho_{\mathrm{G}}\cdots\}$ is the same weighted sum of inner products as mention before and x, x' being position-imaginary-time four vectors. Since the temperature single-particle Green's function is not a function of time, it is only possible to directly extract from it observables which neither dependent on time, that is, thermodynamical properties. In order to obtain time dependent properties, one must first relate the temperature Green's

function to a real-time Green's function. This is something which wont be of importance to this thesis and thus not discussed. From here on we will stick to the finite temperature formalism and whenever a Green's function is mention it will be understood that a temperature Green's function intended.

Assuming the Hamiltonian in the Schrödinger picture is time independent, and also such that it commutates with the momentum operator $\hat{\mathbf{p}}$, then the single-particle thermal Green's function will depend only on the difference $\mathbf{x} - \mathbf{x}'$ and $\tau - \tau'$. For the purpose of this thesis it is also sufficient to further assume that the spin dependency of the Green's function might be factored out as

$$\mathcal{G}_{\alpha\beta}(\mathbf{x}, \tau) = \delta_{\alpha\beta}\, \mathcal{G}(\mathbf{x}, \tau)\,. \tag{2.10}$$

Here we have transformed the parameters $\mathbf{x} - \mathbf{x}' \to \mathbf{x}$ and $\tau - \tau' \to \tau$ for a shorter notation. Since the spin dependency is trivial, we will drop it and from now on refer to the single-particle Green's function as $\mathcal{G}(\mathbf{x}, \tau)$.

For reasons to become evident later, it is necessary to work within the momentum-imaginary-time representation rather than the position-imaginary-time representation. Hopefully it should not come as a surprise, that in the limit of infinite system size, the single-particle Greens function in momentum space is obtain by the Fourier transform,

$$\mathcal{G}(\mathbf{x}, \tau) = \int \frac{\mathrm{d}^3 k}{(2\pi)^3}\, e^{i\mathbf{k}\cdot\mathbf{x}}\, \mathcal{G}(\mathbf{k}, \tau)\,. \tag{2.11}$$

For the sake of the thesis it is not necessary to keep the ground state ensemble of the system completely general. So in order to simplify the following analysis it is permissible to assume the ground state to be empty (do we also need to assume $T = 0$?) (this is actually the ground state to be used in the upcoming diagrammatic Monte Carlo algorithm (better word needed)). This implies that $\mathrm{Tr}\{\cdots\} \to \langle \mathrm{vac}| \cdots |\mathrm{vac}\rangle$.

Assuming the system to be cubic, with a finite volume $V = l^3$, accompanied also by periodic boundary conditions, the single-particle wave functions of the momentum eigenstates are found to be

$$\psi_{\mathbf{k}}(\mathbf{x}) = \frac{e^{i\mathbf{k}\cdot\mathbf{x}}}{\sqrt{V}}\,. \tag{2.12}$$

The components of the allowed momenta are then

$$\mathbf{k}_i = \frac{2\pi}{l} n_i\,; \quad n_i = 0, \pm 1, \pm 2, \cdots\,. \tag{2.13}$$

Using this set of quantum numbers in the definition (2.5) of the field operator, it is possible to rewrite

$$\begin{aligned}\mathcal{G}(\mathbf{x},\tau) &= \sum_{\mathbf{k},\mathbf{p}} \psi_{\mathbf{k}}(\mathbf{x})\psi^{\dagger}_{\mathbf{p}}(\mathbf{0})\langle \mathrm{vac}|\hat{\rho}_{\mathrm{G}}\, T_{\tau}[\hat{c}_{\mathbf{k}}(\tau)\hat{c}^{\dagger}_{\mathbf{p}}(0)]|\mathrm{vac}\rangle \\ &= \theta(\tau)\sum_{\mathbf{k},\mathbf{p}} \psi_{\mathbf{k}}(\mathbf{x})\psi^{\dagger}_{\mathbf{p}}(\mathbf{0})\delta_{\mathbf{k},\mathbf{p}}\langle \mathrm{vac}|\hat{c}_{\mathbf{k}}(\tau)\hat{c}^{\dagger}_{\mathbf{k}}(0)|\mathrm{vac}\rangle \\ &= \theta(\tau)\sum_{\mathbf{k}} \psi_{\mathbf{k}}(\mathbf{x})\psi^{\dagger}_{\mathbf{k}}(\mathbf{0})\langle \mathrm{vac}|\hat{c}_{\mathbf{k}}(\tau)\hat{c}^{\dagger}_{\mathbf{k}}(0)|\mathrm{vac}\rangle \\ &= \theta(\tau)\frac{1}{V}\sum_{\mathbf{k}} e^{i\mathbf{k}\cdot\mathbf{x}}\langle \mathrm{vac}|\hat{c}_{\mathbf{k}}(\tau)\hat{c}^{\dagger}_{\mathbf{k}}(0)|\mathrm{vac}\rangle\end{aligned} \tag{2.14}$$

remove the usage of theta perhaps.

Taking the limit $l \to \infty$ the separation between the eigen-momenta become infinitesimally small, and one should thus replace with

$$\frac{1}{V}\sum_{\mathbf{k}} \cdots \to \int \frac{\mathrm{d}^3 k}{(2\pi)^3} \cdots . \tag{2.15}$$

By finally comparing expression (2.14) with the definition of $\mathcal{G}(\mathbf{k},\tau)$ (2.11), we identify

$$\mathcal{G}(\mathbf{k},\tau) = \theta(\tau)\langle \mathrm{vac}|\hat{c}_{\mathbf{k}}(\tau)\hat{c}^{\dagger}_{\mathbf{k}}(0)|\mathrm{vac}\rangle\,. \tag{2.16}$$

In order to demonstrate some important properties of $\mathcal{G}(\mathbf{k},\tau)$ the unity operator $\hat{\mathbb{1}} = \sum_{\nu} |\nu\rangle\langle\nu|$, constructed in terms of the complete set of eigenstates $\{|\nu(\mathbf{k})\rangle\}$ to the grand canonical Hamiltonian $\hat{K}\,|\nu(\mathbf{p})\rangle = E_{\nu}(\mathbf{p})\,|\nu(\mathbf{p})\rangle$, is inserted into expression (2.16). By recalling that the imaginary-time evolution of the annihilation operator in the modified Heisenberg picture is given by $\hat{c}_{\mathbf{k}}(\tau) = e^{\hat{K}\tau}\,\hat{c}_{\mathbf{k}}(0)\,e^{-\hat{K}\tau}$ the expression then boils down to[2]

$$\mathcal{G}(\mathbf{k},\tau) = \theta(\tau)\sum_{\nu} |\langle\nu|\hat{c}^{\dagger}_{\mathbf{k}}|\mathrm{vac}\rangle|^2 e^{-(E_{\nu}-E_{\mathrm{vac}})\tau}\,. \tag{2.17}$$

Here we have used that E_{vac} is the vacuum (!?) energy, i.e. $\hat{K}\,|\mathrm{vac}\rangle = E_{\mathrm{vac}}\,|\mathrm{vac}\rangle$. It happens to be so, that in the model to be used $E_0 = 0$, hence from here on E_{vac} will be omitted. Rather than working with some unknown set $\{\nu\}$, it is more convenient to parametrize using the frequency. This is done by introducing the spectral density function

$$g_{\mathbf{k}}(\omega) \equiv \sum_{\nu} \delta(\omega - E_{\nu})\,|\langle\nu|\hat{c}^{\dagger}_{\mathbf{k}}|\mathrm{vac}\rangle|^2\,, \tag{2.18}$$

through which the single-particle Green's function is expressed as

$$\mathcal{G}(\mathbf{k},\tau) = \int g_{\mathbf{k}}(\omega)\, e^{-\omega\tau}\, \mathrm{d}\omega\,. \tag{2.19}$$

according to [2] the spectral density is one sided, why is this? Clearly there exist stable states for which $E_\nu < 0$.

Assuming the single-particle Green's function to be that of an electron ($\hat{c}_{\mathbf{k}} \to \hat{a}_{\mathbf{k}}$), the factor $|\langle\nu|\hat{a}^\dagger_{\mathbf{k}}|\mathrm{vac}\rangle|^2$ is nothing more than the overlap of that particular eigenstate of $\hat{K}$ onto a free electron with momentum $\mathbf{k}$, i.e. $|\mathbf{k}\rangle$. If there exist a stable eigenstate $|\xi_{\mathbf{k}}\rangle$ with energy $E(\mathbf{k})$, the spectral function should contain the term $|\langle\xi_{\mathbf{k}}|\mathbf{k}\rangle|^2\,\delta(\omega - E(\mathbf{k}))$. Being a stable state, the energy $E(\mathbf{k})$ is lower than the corresponding energy of any other possible eigenstate. According to (2.19), at imaginary-times $\tau \to \infty$, the sole contribution to the single-particle Green's function should come from this stable state. That is,

$$\mathcal{G}(\mathbf{k},\tau\to\infty) = Z_0^{\mathbf{k}} e^{-E(\mathbf{k})\tau}\,, \tag{2.20}$$

where the notation $Z_0^{\mathbf{k}} = |\langle\xi_{\mathbf{k}}|\mathbf{k}\rangle|^2$ has been used.

2.2.2 Free (bare?) single-particle Green's function

Carry out this derivation without any assumptions on the system at hand.

A state of a particle obeying a Hamiltonian consisting solely of a kinetic one-body operator, i.e. $\hat{K}_0 = \sum_\nu \epsilon_\nu \hat{c}^\dagger_\nu \hat{c}_\nu$, is said to be free (another word perhaps?). Here the energy ϵ_ν is known from solving the corresponding problem in first-quantization. There is no need to keep a higher level of generality here than done previously, so using those same assumptions expression (2.17) might be reused,

$$\mathcal{G}_0(\mathbf{k},\tau) = \theta(\tau)\sum_\nu |\langle\nu|\hat{c}^\dagger_{\mathbf{k}}|\mathrm{vac}\rangle|^2 e^{-\epsilon_\nu\tau}\,. \tag{2.21}$$

However, this time the set of eigenstates $\{|\nu\rangle\}$ are known to be the momentum eigenstates $\{|\mathbf{p}\rangle\}$ since the Hamiltonian was said to commutate with the momentum operator. Using the orthonormality amongst those states, the expression of the free single-particle Green's function simplifies to

$$\mathcal{G}_0(\mathbf{k},\tau) = \theta(\tau)\, e^{-\epsilon(\mathbf{k})\,\tau}\,. \tag{2.22}$$

Here it is once again assumed that the system is infinite so that $\mathbf{k}$ is treated as being continuous.

2.3 Derivation of the Fröhlich Hamiltonian

What will happen to a dielectric medium if one introduces a charged particle, and how will this particle react to changes in the dielectric medium? These are questions which Herbert Fröhlich answered in his 1954 paper *Electrons in lattice fields*[3]. In

this section we will outline the original derivation but also look into some details relevant to us.

mention something out of the polaron book?

2.3.1 Classical picture

The model of interest to this thesis is the following. Consider a diatomic crystal, e.g. rock salt. Such a crystal is made up out of ions which pairwise have a zero net charge. This is depicted in figure 2.1 below. Introducing a free electron into such a crystal, the electron will polarize the crystal due to it exerting an electric field. This sort of polarization may be described by a displacement vector for each lattice point. However, to simplify matters, it is preferred to treat this displacement vector as a continuous vector field.

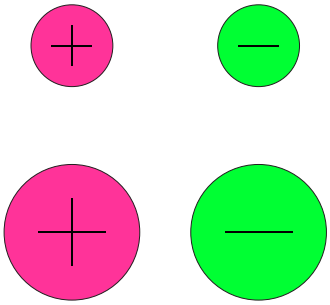

(a) The filled circles illustrate four types of charges. The color represent the charge sign; the ones to the left are positively charged and the ones to the right are negatively charged. The quantity of charge is represented by the size; the charges have the same charge quantity within each row, but the ones in the top row have a weaker charge than the ones in the bottom row.

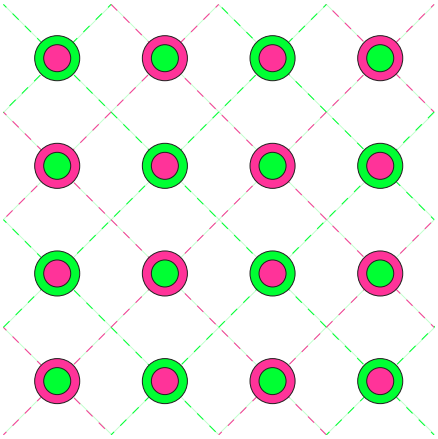

(b) A layer of a diatomic crystal. This particular crystal has a face-centered cubic structure.

Figure 2.1

If we first consider a steady state situation, the polarization is determined solely by the dielectric permittivity ε_r. Introducing the electric displacement field $\mathbf{D} = \mathbf{E} + 4\pi\mathbf{P}$ (CGS units) for which the source is the free electron, this may be thought

of as the external electrical field. If our electron is at position $\mathbf{r}_\mathrm{e}$, the $\mathbf{D}$-field at a position r is given by the usual

$$\mathbf{D}(\mathbf{r}, \mathbf{r}_\mathrm{e}) = -\nabla \frac{Q}{|\mathbf{r} - \mathbf{r}_\mathrm{e}|} \tag{2.23}$$

so that

$$\nabla \cdot \mathbf{D}(\mathbf{r}, \mathbf{r}_\mathrm{e}) = 4\pi q\, \delta(\mathbf{r} - \mathbf{r}_\mathrm{e})\,. \tag{2.24}$$

Here Q is the charge of the electron and the second equality is to be thought of as valid inside of an integral. In agreement with the definition of the $\mathbf{D}$-field we may also define the electric field due to the bound charges as $\mathbf{E}_\mathrm{bound} = -4\pi\mathbf{P}$ since $\mathbf{D} = \mathbf{E} + 4\pi\mathbf{P} = \mathbf{E} - \mathbf{E}_\mathrm{bound} \equiv \mathbf{E}_\mathrm{free}$.

The interaction energy, which is minimised when the $\mathbf{D}$-field is parallel to the polarisation, is given by (why!? Dipole something?)

$$E_\mathrm{int} = -\int_V \mathbf{D}(\mathbf{r}, \mathbf{r}_\mathrm{e}) \cdot \mathbf{P}(\mathbf{r})\, \mathrm{d}^3 r\,. \tag{2.25}$$

By utilising the scalar potential of the bound electric field $\mathbf{E}_\mathrm{bound}(r) = -\nabla\Phi(\mathbf{r})$ along with the quantities defined above, this interaction energy may be rewritten as

$$\begin{aligned}
E_\mathrm{int} &= -\frac{1}{4\pi}\int_\Omega \mathbf{D}(\mathbf{r}, \mathbf{r}_\mathrm{e}) \cdot \nabla\Phi(\mathbf{r})\, \mathrm{d}^3 r \\
&= -\frac{1}{4\pi}\int_{\Omega\setminus V_\varepsilon} \mathbf{D}(\mathbf{r}, \mathbf{r}_\mathrm{e}) \cdot \nabla\Phi(\mathbf{r})\, \mathrm{d}^3 r - \frac{1}{4\pi}\int_{V_\varepsilon} \mathbf{D}(\mathbf{r}, \mathbf{r}_\mathrm{e}) \cdot \nabla\Phi(\mathbf{r})\, \mathrm{d}^3 r \\
&= -\frac{1}{4\pi}\int_{\Omega\setminus V_\varepsilon} \nabla \cdot [\Phi(\mathbf{r})\mathbf{D}(\mathbf{r}, \mathbf{r}_\mathrm{e})]\, \mathrm{d}^3 r + \underbrace{\frac{1}{4\pi}\int_{\Omega\setminus V_\varepsilon} \Phi(\mathbf{r})\nabla \cdot \mathbf{D}(\mathbf{r}, \mathbf{r}_\mathrm{e})\, \mathrm{d}^3 r}_{0} + \underbrace{\frac{q}{4\pi}\int_{V'_\varepsilon} \frac{1}{r^2}\frac{\partial\Phi(\mathbf{r} + \mathbf{r}_\mathrm{e})}{\partial r}\, \mathrm{d}^3 r}_{\to 0 \text{ as } \varepsilon \to 0} \\
&= \frac{Q}{4\pi}\int_{-\partial V'_\varepsilon} \Phi(\mathbf{r} + \mathbf{r}_\mathrm{e})\nabla\frac{1}{r} \cdot \mathrm{d}^2\mathbf{r} \\
&= Q\,\Phi(\mathbf{r}_\mathrm{e})
\end{aligned} \tag{2.26}$$

Here we have both assumed that $\Phi(\mathbf{r})$ has a continuous first derivative as well as $\Phi(\mathbf{r})\mathbf{D}(\mathbf{r}, \mathbf{r}_\mathrm{e}) \simeq 0$ on the boundary $\mathbf{r} \in \partial\Omega$. In order to use the divergence theorem the singularity at $\mathbf{r}_\mathrm{e}$ has been isolated in a spherical volume V_ε centered at $\mathbf{r}_\mathrm{e}$ with radius $\varepsilon \to 0$.

Next we bring back the time dependence and no longer consider a situation which is in steady state. Since each lattice point in our crystal is occupied by a ion, the dynamic in our system is characterized by two time scales. That is, the time it takes to displace the bound electrons relative their nuclei (deformation of ion) and the time it takes to displace the nucleus relative the lattice (deformation of lattice structure). These two types of deformation are illustrated in figure 2.2 below. Since the electrons are significantly lighter than their nucleus, the ion deformation time

should thus be much smaller than the time it takes to deformation the lattice. Denoting these times as t_{uv} and t_{ir} respectively we thus have that $t_{\text{uv}} \ll t_{\text{ir}}$ which corresponds to $\omega_{\text{uv}} \gg \omega_{\text{ir}}$. The subscripts of course indicate that frequencies lie in the ultraviolet and infrared region respectively. The total deformation is due to these two deformation so that $\mathbf{P} = \mathbf{P}_{\text{ir}} + \mathbf{P}_{\text{uv}}$.

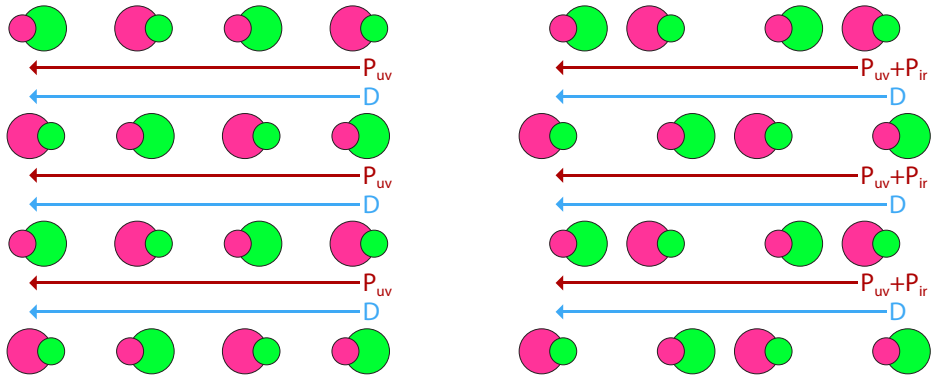

(a) Deformation of the ions.

(b) Deformation of the lattice.

Figure 2.2

It is further reasonable to assume that each of these contributions behave as a driven harmonic oscillator, that is

$$\ddot{\mathbf{P}}_{\text{ir}}(\mathbf{r}) + \omega_{\text{ir}}^2 \mathbf{P}_{\text{ir}}(\mathbf{r}) = \frac{\mathbf{D}(\mathbf{r}, \mathbf{r}_{\text{e}})}{\gamma} , \quad \ddot{\mathbf{P}}_{\text{uv}}(\mathbf{r}) + \omega_{\text{uv}}^2 \mathbf{P}_{\text{uv}}(\mathbf{r}) = \frac{\mathbf{D}(\mathbf{r}, \mathbf{r}_{\text{e}})}{\delta} . \tag{2.27}$$

Here γ and δ are constants to be determined in what follows. First we must once again quickly consider a static situation. Here the static dielectric constant ϵ would give us $\mathbf{D} = \epsilon \mathbf{E}$ which we could use together with the previously stated definition of the $\mathbf{D}$-field to relate $\mathbf{P}$ and $\mathbf{D}$ as

$$4\pi \mathbf{P}(\mathbf{r}) = (1 - 1/\epsilon)\mathbf{D}(\mathbf{r}, \mathbf{r}_{\text{e}}) . \tag{2.28}$$

Next we once again turn back time and utilize the high frequency dielectric constant ϵ_∞, defined by $\mathbf{D} = \epsilon_\infty \mathbf{E}$, under the assumption that the frequency ω_∞ of the external field satisfies $\omega_{\text{uv}} \gg \omega_\infty \gg \omega_{\text{ir}}$. The latter is simply implying that the free electron in our crystal is moving slowly (Fast enough for the IR polarization not to follow, right!?). This tells us that the UV-part of the polarization will follow the changes in the $\mathbf{D}$-field nearly adiabatically whilst the IR-part wont have time adapt to the changes and may thus be thought of as a negligible constant field in

comparison, that is, $\mathbf{P} \simeq \mathbf{P}_{\text{uv}}$. Using this together with the relation of $\mathbf{D}$ and $\mathbf{E}$ through ϵ_∞ we find, in similarity to (2.28),

$$4\pi\mathbf{P}_{\text{uv}}(\mathbf{r}) = (1 - 1/\epsilon_\infty)\mathbf{D}(\mathbf{r}, \mathbf{r}_{\text{e}})\,. \tag{2.29}$$

Taking the difference between (2.28) and (2.29) we find a similar equation for $\mathbf{P}_{\text{ir}}$

$$4\pi\mathbf{P}_{\text{ir}}(\mathbf{r}) = (1/\epsilon_\infty - 1/\epsilon)\mathbf{D}(\mathbf{r}, \mathbf{r}_{\text{e}})\,. \tag{2.30}$$

Noting that $\ddot{\mathbf{P}}_{\text{uv}} \approx \omega_\infty^2\,\mathbf{P}_{\text{uv}} \ll \omega_{\text{uv}}^2\,\mathbf{P}_{\text{uv}}$ and assuming that $\mathbf{P}_{\text{ir}}$ is seemingly constant at timescales of length $1/\omega_{\text{ir}}$, equation (2.27) simplifies into (in the original derivation they simply compared using steady state where the time derivatives obviously are zero, but this must be equivalent due to $\omega_{\text{uv}} \gg \omega_\infty \gg \omega_{\text{ir}}$?)

$$\omega_{\text{ir}}^2\,\mathbf{P}_{\text{ir}}(\mathbf{r}) = \frac{\mathbf{D}(\mathbf{r}, \mathbf{r}_{\text{e}})}{\gamma}\,, \quad \omega_{\text{uv}}^2\,\mathbf{P}_{\text{uv}}(\mathbf{r}) = \frac{\mathbf{D}(\mathbf{r}, \mathbf{r}_{\text{e}})}{\delta}\,. \tag{2.31}$$

Comparing this equation to (2.29) and (2.30) we find the value of γ and δ in terms of know material properties

$$\frac{1}{\gamma} = \frac{\omega_{\text{ir}}^2}{4\pi}\left(\frac{1}{\epsilon_\infty} - \frac{1}{\epsilon}\right)\,, \quad \frac{1}{\delta} = \frac{\omega_{\text{uv}}^2}{4\pi}\left(1 - \frac{1}{\epsilon_\infty}\right)\,. \tag{2.32}$$

Having obtained the equation of motion for the two types of polarisation, our next task is to find the one for the free electron. Since the electron had low in kinetic energy, we may without hesitation treat it in the non relativistic limit. The only force acting on the electron is due to the bound electric field, that is $\mathbf{F}(\mathbf{r}_{\text{e}}) = q\mathbf{E}_{\text{bound}}(\mathbf{r}_{\text{e}}) = -q\nabla\Phi(\mathbf{r}_{\text{e}})$. Thus $m\ddot{\mathbf{r}}_{\text{e}} = \dot{\mathbf{p}}_{\text{e}} = -q\nabla\Phi(\mathbf{r}_{\text{e}})$ where m is an effective mass which in general is different from the electronic mass m_{e}. By treating $\mathbf{p}_{\text{e}}$, $\mathbf{P}_{\text{uv}}(\mathbf{r})$ and $\mathbf{P}_{\text{ir}}(\mathbf{r})$ as variables, we may by combining all the equation of motions derived above together with expression for the interaction energy (2.26) form the Lagrangian

$$\begin{aligned} L = {} & \frac{\gamma}{2}\int\left[\dot{\mathbf{P}}_{\text{ir}}^2(\mathbf{r}) - \omega_{\text{ir}}^2\,\mathbf{P}_{\text{ir}}^2(\mathbf{r})\right]\mathrm{d}^3r + \frac{\delta}{2}\int\left[\dot{\mathbf{P}}_{\text{uv}}^2(\mathbf{r}) - \omega_{\text{uv}}^2\,\mathbf{P}_{\text{uv}}^2(\mathbf{r})\right]\mathrm{d}^3r \\ & + \int\mathbf{D}(\mathbf{r}, \mathbf{r}_{\text{e}})\cdot\left[\mathbf{P}_{\text{ir}}(\mathbf{r}) + \mathbf{P}_{\text{uv}}(\mathbf{r})\right]\mathrm{d}^3r + \frac{\mathbf{p}_{\text{e}}^2}{2m} \end{aligned} \tag{2.33}$$

and by a Legendre transformation, the Hamiltonian

$$\begin{aligned} H = {} & \frac{\gamma}{2}\int\left[\dot{\mathbf{P}}_{\text{ir}}^2(\mathbf{r}) + \omega_{\text{ir}}^2\,\mathbf{P}_{\text{ir}}^2(\mathbf{r})\right]\mathrm{d}^3r + \frac{\delta}{2}\int\left[\dot{\mathbf{P}}_{\text{uv}}^2(\mathbf{r}) + \omega_{\text{uv}}^2\,\mathbf{P}_{\text{uv}}^2(\mathbf{r})\right]\mathrm{d}^3r \\ & - \int\mathbf{D}(\mathbf{r}, \mathbf{r}_{\text{e}})\cdot\left[\mathbf{P}_{\text{ir}}(\mathbf{r}) + \mathbf{P}_{\text{uv}}(\mathbf{r})\right]\mathrm{d}^3r + \frac{\mathbf{p}_{\text{e}}^2}{2m}\,. \end{aligned} \tag{2.34}$$

Since the UV-part of the polarisation follows the external field nearly adiabatically, the dynamic solution $\mathbf{P}_{\text{uv}}$ is approximatively the statical one with respect to

current $\mathbf{D}$-field. Because of this $\mathbf{P}_{\rm uv}$ will only contribute to the Hamiltonian with a constant and may thus be removed from the theory giving rise only to an energy shift.

Next we observe that the integrals in the expressions above are divergent since $\mathbf{P}_{\rm ir}$ according to (2.29) and (2.30) are proportional to the $\mathbf{D}$-field which is singular at $\mathbf{r} = \mathbf{r}_{\rm e}$. However this divergence is a resulted from us disregarding the atomic structure when interpreting the displacements as a continuous vector field. To resolve this one should express the polarisation in a Fourier series and omit terms with a wave length smaller than that of the lattice constant. Hence we need not to worry about this divergence.

Further more it is useful to introduce here a complex vector field $\mathbf{B}$,

$$\mathbf{B}(\mathbf{r}) = \sqrt{\frac{\gamma\omega_{\rm ir}}{2}}\left[\mathbf{P}_{\rm ir}(\mathbf{r}) + \frac{i}{\omega_{\rm ir}}\dot{\mathbf{P}}_{\rm ir}(\mathbf{r})\right], \quad \mathbf{B}^\dagger(\mathbf{r}) = \sqrt{\frac{\gamma\omega_{\rm ir}}{2}}\left[\mathbf{P}_{\rm ir}(\mathbf{r}) - \frac{i}{\omega_{\rm ir}}\dot{\mathbf{P}}_{\rm ir}(\mathbf{r})\right]. \tag{2.35}$$

Here we have also dropped the subscript of $\omega_{\rm ir}$ since $\omega_{\rm uv}$ no longer appears in our theory. The reasons to why one prefer to work with $\mathbf{B}$ rather than $\mathbf{P}_{\rm ir}$ will be evident later. With this our now non-divergent Hamiltonian becomes,

$$H = \frac{1}{2}m\dot{\mathbf{r}}_{\rm e}^2 + \omega\int \mathbf{B}^\dagger(\mathbf{r})\cdot\mathbf{B}(\mathbf{r})\,\mathrm{d}^3r - \sqrt{\frac{1}{2\gamma\omega}}\int \mathbf{D}(\mathbf{r},\mathbf{r}_{\rm e})\cdot\left[\mathbf{B}(\mathbf{r}) + \mathbf{B}^\dagger(\mathbf{r})\right]\mathrm{d}^3r\,. \tag{2.36}$$

Using a periodic boundary condition over a cube of volume $V = l^3$, $\mathbf{B}$ might be expressed by the Fourier series

$$\mathbf{B}(\mathbf{r}) = \sum_{\mathbf{q}} \frac{\mathbf{q}}{q}\, b_{\mathbf{q}}\, \frac{e^{i\mathbf{q}\cdot\mathbf{r}}}{V}, \quad \mathbf{B}^\dagger(\mathbf{r}) = \sum_{\mathbf{q}} \frac{\mathbf{q}}{q}\, b_{\mathbf{q}}^\dagger\, \frac{e^{-i\mathbf{q}\cdot\mathbf{r}}}{V} \tag{2.37}$$

with

$$\mathbf{q}_i = \frac{2\pi}{l}n_i\,; \quad n_i = 0,\, \pm1,\, \pm2, \cdots,\, \pm N_{\rm cut} \tag{2.38}$$

Refer to these mentioned earlier. However you need to introduce $N_{\rm cut}$.

Here $i = x, y, z$, $|\mathbf{q}| = q$ and the cutoff magnitude $q_{\rm cut} = 2\pi N_{\rm cut}/l$ is inversely proportional to the lattice constant in accordance to what was discussed earlier ($a \lesssim \lambda = 2\pi/k \to k \lesssim a$ right!?) (to write: $q_{\rm cut}$ since we are only looking at the IR-part which is du to lattice deformations at length scales $\propto a$). Also defining a scalar potential for the IR-part of the polarization as $4\pi\mathbf{P}_{\rm ir} = \nabla\Phi_{\rm ir}$ we may, by using equation (2.26), express the interaction energy between $\mathbf{D}$ and $\mathbf{P}_{\rm ir}$ as $Q\,\Phi_{\rm ir}(\mathbf{r}_{\rm e})$. Using (2.35, 2.37) together with $\Phi_{\rm ir}$ the expression for the Hamiltonian becomes

$$H = \frac{\mathbf{p}_e^2}{2m} + \omega \sum_{\mathbf{q}} b_{\mathbf{q}}^\dagger b_{\mathbf{q}} + \frac{1}{V} \sum_{\mathbf{q}} V(q) \left[b_{\mathbf{q}}^\dagger \, e^{-i\mathbf{q}\cdot\mathbf{r}_e} - b_{\mathbf{q}} \, e^{i\mathbf{q}\cdot\mathbf{r}_e} \right] , \tag{2.39}$$

where we have substituted using

$$V(q) = i \left(2\sqrt{2}\pi\alpha \right)^{1/2} \left(\frac{\omega^3}{m} \right)^{1/4} \frac{1}{q} \tag{2.40}$$

and introduced the interaction parameter

$$\alpha = \frac{1}{2} \left(\frac{1}{\epsilon_\infty} - \frac{1}{\epsilon} \right) \sqrt{\frac{2m}{\omega}} Q^2 \, . \tag{2.41}$$

Here it seems as if the interaction part of the Hamiltonian is ill behaved due to the $\mathbf{q} = \mathbf{0}$ term of the sum. This is a result from the periodic boundary condition imposed on our system. Originally the system contained only one free electron. With a periodic boundary condition however, the system now consists of an infinite number of copies of the cube with volume V, each containing a free electron. These electrons interact with one another due to the long range Coulomb repulsion. To avoid this behaviour when periodically continuing the system, one should introduce in each cube a charge density of $-Q/V$. Doing this would give rise to an attractive Coulomb force which for each electron would cancel the Coulomb repulsion. Such an interaction would exactly cancel the ill behaved $\mathbf{q} = \mathbf{0}$ term in the interaction part of the Hamiltonian since the only difference would be the sign of the charge, i.e $Q \to -Q$.

2.3.2 Quantisation

Having sorted out these details we are ready to quantise the Hamiltonian. To do so the first step is to symmetrise $b_{\mathbf{q}}^\dagger b_{\mathbf{q}} = (b_{\mathbf{q}}^\dagger b_{\mathbf{q}} + b_{\mathbf{q}} b_{\mathbf{q}}^\dagger)/2$ (why? source needed.). Next up, using[4]

$$\dot{q} = \frac{\delta H}{\delta p} \, , \quad \dot{p} = -\frac{\delta H}{\delta q} \tag{2.42}$$

together with (2.27, 2.34) it is easy to verify that $\mathbf{P}_{\text{ir}}$ and $\gamma \dot{\mathbf{P}}_{\text{ir}}$ or equivalent, $(b_{\mathbf{q}}^\dagger + b_{\mathbf{q}})/\sqrt{2\gamma\omega}$ and $i(b_{\mathbf{q}}^\dagger - b_{\mathbf{q}})\sqrt{\gamma\omega/2}$ for each $\mathbf{q}$, are conjugate variables (how do we arrive at the final set of conjugate variables? Using some sort of transformation perhaps? Try find in the book by Egor.). By promoting to operators $b_{\mathbf{q}} \to \hat{b}_{\mathbf{q}}$, $\mathbf{r}_e \to \hat{\mathbf{r}}_e$, $\mathbf{p}_e \to \hat{\mathbf{p}}_e$ and imposing Bose statistics (How do we know this? spinless?) onto the conjugate variables,

$$i\delta_{\mathbf{q},\mathbf{k}} = \frac{i}{2} [\hat{b}_{\mathbf{q}}^\dagger + \hat{b}_{\mathbf{q}}, \, \hat{b}_{\mathbf{k}}^\dagger - \hat{b}_{\mathbf{k}}]/2 \tag{2.43}$$

Perhaps V is important for the equation above?

we obtain $[b_{\mathbf{q}}, b^\dagger_{\mathbf{k}}] = \delta_{\mathbf{q},\mathbf{k}}$ and $[b_{\mathbf{q}}, b_{\mathbf{k}}] = 0$ (really, they follow?). Using the first of these to rewrite $(\hat{b}^\dagger_{\mathbf{q}}\hat{b}_{\mathbf{q}} + \hat{b}_{\mathbf{q}}\hat{b}^\dagger_{\mathbf{q}})/2 = \hat{b}^\dagger_{\mathbf{q}}\hat{b}_{\mathbf{q}} + \frac{1}{2}$ the Hamiltonian, in quantised form, becomes

$$\hat{H} = \frac{\hat{\mathbf{p}}_{\mathrm{e}}^2}{2m} + \omega \sum_{\mathbf{q}} \hat{b}^\dagger_{\mathbf{q}}\hat{b}_{\mathbf{q}} + \frac{1}{V}\sum_{\mathbf{q}} V(q)\left(\hat{b}^\dagger_{\mathbf{q}}\, e^{-i\mathbf{q}\cdot\hat{\mathbf{r}}_{\mathrm{e}}} - \hat{b}_{\mathbf{q}}\, e^{i\mathbf{q}\cdot\hat{\mathbf{r}}_{\mathrm{e}}}\right) . \tag{2.44}$$

Here we have omitted the zero point energy $\omega\sum_{\mathbf{q}}\frac{1}{2}$ of the oscillating ions. At this stage it has become evident that $\hat{b}^\dagger_{\mathbf{q}}$ and $\hat{b}_{\mathbf{q}}$ may be recognised[3] as the creation and annihilation operator of a harmonic oscillator of mass M, with position and momentum coordinates

$$\hat{q}_{\mathbf{k}} = \sqrt{\frac{1}{2M\omega}}\left(\hat{b}^\dagger_{\mathbf{k}} + \hat{b}_{\mathbf{k}}\right) , \quad \hat{p}_{\mathbf{k}} = i\sqrt{\frac{M\omega}{2}}\left(\hat{b}^\dagger_{\mathbf{k}} - \hat{b}_{\mathbf{k}}\right) . \tag{2.45}$$

The polarization field $\mathbf{P}_{\mathrm{ir}}$ is in this manner being represented by a set of harmonic oscillators each corresponding to a quantized mode of vibration in the lattice, i.e. a phonon. Since the frequency of the phonons is momentum independent they are said to be dispersionless (right!?). For optical phonons which couple to infrared radiation, this is at low momenta a good approximation as shown in the figure 2.3 below.

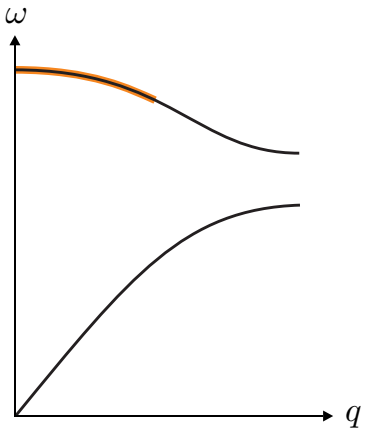

Figure 2.3: The upper and lower curves depict the characteristics of an optical and acoustic dispersion relation respectively. The outlined orange region illustrates were the optical dispersion relation might be approximated as momentum independent.

Having sorted out the quantisation of the **B**-field we turn our attention towards the electron. In order to later expand the interacting theory using Feynman diagrams, we which to represent the free electron by a many-body Fock state instead

of having it represented by a single-body Hilbert state. In order to do this the second quantisation formalism need to utilised. Using the momentum basis as the electronic many-body Fock occupation state with corresponding creation and annihilation operators $\hat{a}^\dagger_{\mathbf{k}}$ and $\hat{a}_{\mathbf{k}}$ respectively, the translation of a one-body operator from first-quantisation to second-quantisation is[1]

$$\hat{O}_2 = \sum_{\mathbf{k},\mathbf{p}} \langle \mathbf{k}|O_1|\mathbf{p}\rangle \hat{a}^\dagger_{\mathbf{k}} \hat{a}_{\mathbf{p}} \,. \tag{2.46}$$

Perhaps move this to a section/subsection about field theory.

Here $\hat{O}_2$ is the second-quantized operator and O_1 is the corresponding first-quantized operator sandwiched between the single-particle Hilbert states $|\mathbf{k}\rangle$, $|\mathbf{p}\rangle$. Mention that these momenta are discretized in the same way as before but without a cutoff. The second-quantized operators then become

$$\frac{\hat{\mathbf{p}}_{\mathrm{e}}^2}{2m} \to \sum_{\mathbf{p}} \frac{p^2}{2m} \hat{a}^\dagger_{\mathbf{p}} \hat{a}_{\mathbf{p}} \,, \quad e^{-i\mathbf{q}\cdot\hat{\mathbf{r}}_{\mathrm{e}}} \to \sum_{\mathbf{p}} \hat{a}^\dagger_{\mathbf{p}-\mathbf{q}} \hat{a}_{\mathbf{p}} \,, \quad e^{i\mathbf{q}\cdot\hat{\mathbf{r}}_{\mathrm{e}}} \to \sum_{\mathbf{p}} \hat{a}^\dagger_{\mathbf{p}+\mathbf{q}} \hat{a}_{\mathbf{p}} \,. \tag{2.47}$$

The form of the second operator follow from

$$\begin{aligned}
\sum_{\mathbf{k},\mathbf{p}} \langle \mathbf{k}|e^{-i\mathbf{q}\cdot\hat{\mathbf{r}}_{\mathrm{e}}}|\mathbf{p}\rangle \hat{a}^\dagger_{\mathbf{k}} \hat{a}_{\mathbf{p}} &= \sum_{\mathbf{k},\mathbf{p}} \langle \mathbf{k}| \left[\int |\mathbf{x}\rangle\langle\mathbf{x}| \, \mathrm{d}^3x\right] e^{-i\mathbf{q}\cdot\hat{\mathbf{r}}_{\mathrm{e}}} \left[\int |\mathbf{y}\rangle\langle\mathbf{y}| \, \mathrm{d}^3y\right] |\mathbf{p}\rangle \hat{a}^\dagger_{\mathbf{k}} \hat{a}_{\mathbf{p}} \\
&= \sum_{\mathbf{k},\mathbf{p}} \hat{a}^\dagger_{\mathbf{k}} \hat{a}_{\mathbf{p}} \int \mathrm{d}^3x \, \frac{e^{-i\mathbf{k}\cdot\mathbf{x}}}{\sqrt{V}} \, e^{-i\mathbf{q}\cdot\mathbf{x}} \, \frac{e^{i\mathbf{p}\cdot\mathbf{x}}}{\sqrt{V}} \\
&= \sum_{\mathbf{k},\mathbf{p}} \hat{a}^\dagger_{\mathbf{k}} \hat{a}_{\mathbf{p}} \, \delta(\mathbf{k}+\mathbf{q}-\mathbf{p}) \\
&= \sum_{\mathbf{p}} \hat{a}^\dagger_{\mathbf{p}-\mathbf{q}} \hat{a}_{\mathbf{p}}
\end{aligned} \tag{2.48}$$

and similarly for the last of the three operators. By substituting this into the Hamiltonian and using that interaction term is symmetric with respect to $\mathbf{q}$, the fully second-quantized Hamiltonian becomes

$$\hat{H} = \sum_{\mathbf{p}} \frac{p^2}{2m} \hat{a}^\dagger_{\mathbf{p}} \hat{a}_{\mathbf{p}} + \omega \sum_{\mathbf{q}} \hat{b}^\dagger_{\mathbf{q}} \hat{b}_{\mathbf{q}} + \frac{1}{V} \sum_{\mathbf{q},\mathbf{p}} V(q) \left(\hat{b}^\dagger_{\mathbf{q}} - \hat{b}_{-\mathbf{q}}\right) \hat{a}^\dagger_{\mathbf{p}-\mathbf{q}} \hat{a}_{\mathbf{p}} \,. \tag{2.49}$$

The grand canonical Hamiltonian $\hat{K}$, which is used extensively in the finite temperature field theory, is obtained by adding chemical potentials to $\hat{H}$. But, since there is no conservation law regarding the number of phonons it must be the case that $\mu_{\mathrm{phonon}} = 0$. Thus

$$\hat{K} = \sum_{\mathbf{p}} \left(\frac{p^2}{2} - \mu \right) \hat{a}^\dagger_{\mathbf{p}} \hat{a}_{\mathbf{p}} + \sum_{\mathbf{q}} \hat{b}^\dagger_{\mathbf{q}} \hat{b}_{\mathbf{q}} + \frac{1}{V} \sum_{\mathbf{q},\mathbf{p}} V(q) \left(\hat{b}^\dagger_{\mathbf{q}} - \hat{b}_{-\mathbf{q}} \right) \hat{a}^\dagger_{\mathbf{p}-\mathbf{q}} \hat{a}_{\mathbf{p}} \tag{2.50}$$

where for convenience $m = \omega = 1$ has been used.

Why does the Hamiltonian not agree with the one in other papers? Are they using another convention of the Fourier transform? In such case, what does this mean for $\hat{b}, \hat{b}^\dagger$?

Where do we assume that the crystal is homogenous/isotropic? Do we even have to do that approximation?

2.4 Perturbation theory

Assume the Hamiltonian to be time-independent in the Schrödinger picture and expressible by the sum $\hat{K} = \hat{K}_0 + \hat{K}_1$. Without the interaction term $\hat{K}_1$ the problem would be exactly solvable. However, if this interaction is weak enough, it is reasonable to treat it perturbatively by expanding with respect to some small interaction parameter α. In order to do so it is necessary to introduce yet a new picture, the interaction picture. In the finite temperature formalism, operators in the interaction picture are related to the ones in the Schrödinger picture through $\hat{O}_{\mathrm{I}}(\tau) = e^{\hat{K}_0 \tau} \hat{O}_{\mathrm{S}} e^{-\hat{K}_0 \tau}$. Within this picture, it is then possible to express the ensemble average of a τ-ordered product of operators using a perturbation series,

$$\begin{gathered} \mathrm{Tr}\{\hat{\rho}_{\mathrm{G}} T_\tau[\hat{A}_{\mathrm{H}}(x_a) \hat{B}_{\mathrm{H}}(x_b) \dots \hat{F}_{\mathrm{H}}(x_f)]\} \\ = \\ \frac{\sum_{n=0}^{\infty} \frac{(-1)^n}{n!} \int_0^\beta \mathrm{d}\tau_1 \dots \int_0^\beta \mathrm{d}\tau_n \, \mathrm{Tr}\left\{ e^{-\beta \hat{K}_0} T_\tau[\hat{K}_1(\tau_1) \dots \hat{K}_1(\tau_n) \, \hat{A}(x_a) \, \hat{B}(x_b) \dots \hat{F}(x_f)] \right\}}{\sum_{n=0}^{\infty} \frac{(-1)^n}{n!} \int_0^\beta \mathrm{d}\tau_1 \dots \int_0^\beta \mathrm{d}\tau_n \, \mathrm{Tr}\left\{ e^{-\beta \hat{K}_0} T_\tau[\hat{K}_1(\tau_1) \dots \hat{K}_1(\tau_n)] \right\}} . \end{gathered} \tag{2.51}$$

In both the nominator and denominator of the expression above, there is the frequently appearing factor

$$\mathrm{Tr}\{e^{-\beta \hat{K}_0} T_\tau[\hat{A} \, \hat{B} \dots \hat{F}]\} . \tag{2.52}$$

It was proved by Matsubara[cite the original paper by Matsubara] that this factor could be rewritten as a sum of permutations of contractions $\hat{A}^{\cdot} \hat{B}^{\cdot} \equiv \mathrm{Tr}\{\hat{\rho}_{\mathrm{G0}} T_\tau[\hat{A} \, \hat{B}]\}$ amongst the operators $\hat{A}$, $\hat{B}$, …, $\hat{F}$. Here $\hat{\rho}_{\mathrm{G0}}$ is the bare statistical operator, defined in accordance with $\hat{\rho}_{\mathrm{G}}$ but having the full Hamiltonian replaced by the non-interacting part only. Since the Hamiltonian usually is written in terms of creation and annihilation operators, it is worth noting that the following contraction

$$\hat{c}_{\mathbf{k}}(\tau)^{\cdot} \hat{c}^\dagger_{\mathbf{k}}(\tau')^{\cdot} = \mathrm{Tr}\{\hat{\rho}_{\mathrm{G0}} T_\tau[\hat{c}_{\mathbf{k}}(\tau) \, \hat{c}^\dagger_{\mathbf{k}}(\tau')]\} = \mathcal{G}_0(\mathbf{k}, \tau) , \tag{2.53}$$

is nothing but the definition of the bare propagator (refer to earlier derivation). Even though there are a multitude of permutations of contractions amongst

the operators in (2.52), most of the turn out to be zero, such as $\hat{c}_{\mathbf{k}}(\tau)^{\cdot}\,\hat{c}_{\mathbf{k}}(\tau')^{\cdot}$, $\hat{c}^{\dagger}_{\mathbf{k}}(\tau)^{\cdot}\,\hat{c}^{\dagger}_{\mathbf{k}}(\tau')^{\cdot}$ and $\hat{c}_{\mathbf{k}}(\tau)^{\cdot}\,\hat{c}^{\dagger}_{\mathbf{p}}(\tau')^{\cdot}$ for $\mathbf{k} \neq \mathbf{p}$. Hence only a small fraction of terms survive, and these are the ones which may be represented pictorially in terms of Feynman diagrams. Also the denominator of (2.51) will serve to precisely cancel out any unconnected parts of diagrams from the nominator. What is left of the perturbations series is then an infinite number of Feynman diagrams which are easily constructed from a set of Feynman rules.

2.4.1 Diagrammatic analysis

In this thesis only the electronic single-particle Green's function will be studied in terms of Feynman diagrams. In order to do this, the operators $\hat{A}\,\hat{B}\,\ldots\,\hat{F}$ in the perturbation series (2.51) should be replaced by $\hat{a}_{\mathbf{k}}\hat{a}^{\dagger}_{\mathbf{k}}$. The constituents of the resulting Feynman diagrams are easily obtained just by analyzing the Hamiltonian (2.50). Using the ground state ensemble of vacuum as promised earlier, the bare electronic and phononic propagators, referred to as $\mathcal{G}_0$ and $\mathcal{D}_0$ respectively, are found to be

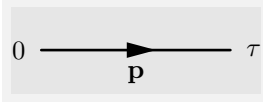

$$= \mathcal{G}_0(\mathbf{p},\tau) = \exp\left\{-\left(\frac{p^2}{2}-\mu\right)\tau\right\} \quad \tau \geq 0\,, \tag{2.54}$$

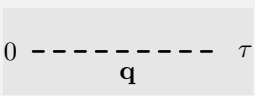

$$= \mathcal{D}_0(\mathbf{q},\tau) = \exp\{-\tau\} \quad \tau \geq 0\,. \tag{2.55}$$

Since any propagator going backwards in time is identically zero, it is possible to use the convention that the momentum is carried in the direction of increased time, which throughout this paper will be to the right. By examining the interaction part of the Hamiltonian, the possible vertices and their contribution are found to be

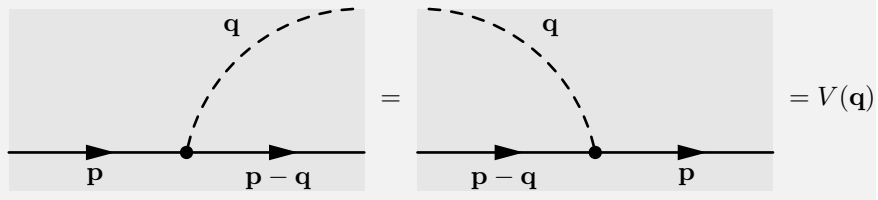

(2.56)

with $V(\mathbf{q})$ as defined in (2.40).

In order to construct the relevant diagrams from these building blocks, the Feynman rules dictate:

1. Draw all topologically distinct diagrams with $2n + 1$ electron lines and n phonon lines.

2. With each particle line associate a factor $\mathcal{G}$ in case of an electron, and $\mathcal{D}$ in case of a phonon.

3. Each vertex contributes with the factor $V(\mathbf{q})$, where $\mathbf{q}$ is the momentum of the connected phonon.

4. Conserve the total momentum at every vertex.

5. The external legs should both be assigned the external momentum $\mathbf{p}$ of the interacting Green's function $\mathcal{G}(\mathbf{p}, \tau)$. The ingoing external leg should start at the imaginary-time 0 and the outgoing external leg should terminate at τ.

6. For each of the n internal momenta, sum over all allowed momentum values.

7. For each of the n internal imaginary-times, integrate from 0 to β.

8. Multiply each diagram with the factor $(-V)^{-n}$.

In this paper the single-particle Green's function will be studied in the limit $V \to \infty$ so that the replacement

$$\frac{1}{V} \sum_{\mathbf{k}} \cdots \to \int \frac{\mathrm{d}^3 k}{(2\pi)^3} \cdots \tag{2.57}$$

should be made in the $\hat{K}_1(\tau)$ factors within the perturbation expansion. Instead of summing over the n internal momenta, there will now be integrals. Also the last one of the Feynman rules should be modified so that multiplicative factor becomes $(-2\pi)^{-3n}$. Further more $T = 0$ will be used and hence the upper bound in the imaginary-time integrals becomes infinite.

Having the ground state ensemble equal to that of vacuum, the propagators become identically zero for negative imaginary-times as stated in (2.54) and (2.55). Because of this the contribution from diagrams containing tadpoles, electron loops and similar structures to those depicted in figure 2.4 vanishes.

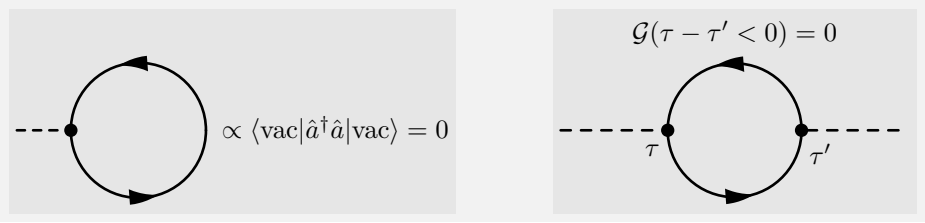

Figure 2.4: caption me plx!

Then the only contributing diagrams are those where all electron propagators follow after one another in a line, and phonon propagators spawn and die on the

vertices in this line. That is,

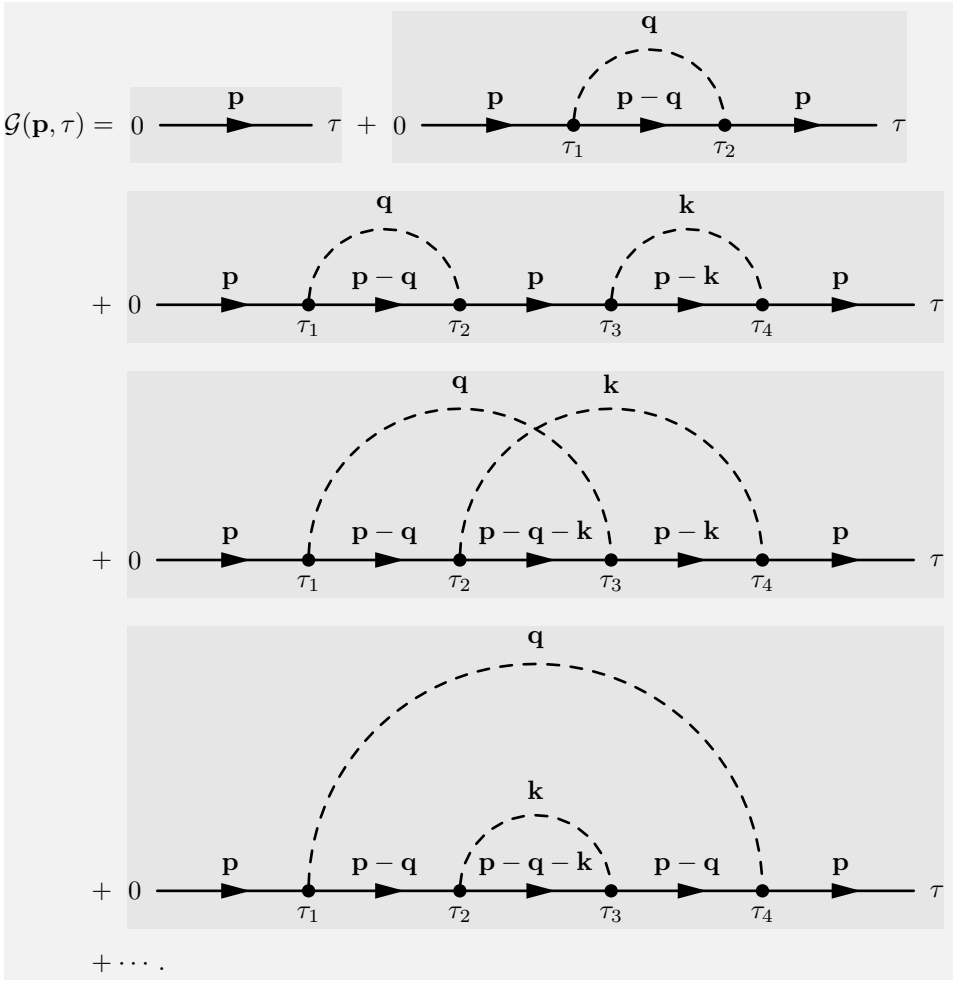

(2.58)

Number of diagrams at each order $\frac{(2n)!}{n!2^n}$

Since there is no preferred direction of the external momentum $\mathbf{p}$, the Green's function will depend only upon the magnitude $p = |\mathbf{p}|$, i.e. $\mathcal{G} = \mathcal{G}(\alpha, \mu, p, \tau)$.

It is obvious that theses diagrams only contribute if the times are ordered chronologically, i.e. $0 = \tau_0 \leq \tau_1 \leq \tau_2 \leq \cdots \leq \tau_{2n-1} = \tau$. Because if this was not the case at least one propagator would propagate backwards in time and contribute with a factor of zero. Thus it is only meaningful to carry out the integrals such that this chronologization constraint is fulfilled.

Another important property of these diagrams is that they all carry a positive definite contribution to $\mathcal{G}$. This since the value of a propagator always is larger than or equal to zero, and the sign from the factor $(-2\pi)^{-3n}$ cancel the i^{2n} contained within $V(\mathbf{q})^{2n}$.

2.4.2 Dyson equation

Working at zero temperature allows for a full Fourier representation of the single-particle Green's function, i.e.

$$G(\mathbf{x}, \tau) = \frac{1}{(2\pi)^4} \int \mathrm{d}^3 k \int \mathrm{d}\omega \, e^{i(\mathbf{k}\cdot\mathbf{x} - \omega\tau)} G(\mathbf{k}, \omega) \, ; \quad G = \mathcal{G},\, \mathcal{D},\, \mathcal{G}_0,\, \mathcal{D}_0 \, . \tag{2.59}$$

It so happens to be more pleasant working in $\mathbf{k}$-ω space for a lot of reasons but what will be of importance here is the conservation of total four momentum $k = (\omega, \mathbf{k})$ at all vertices in a Feynman diagram. In that way the external legs of a diagram no longer depend upon any internal variables and may then be factored out from the nasty integral expression. Hence it is convenient to define the interacting single-particle Green's function, here depicted as a double line, in terms of the self-energy as

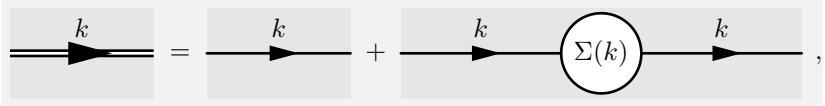

, (2.60)

so that

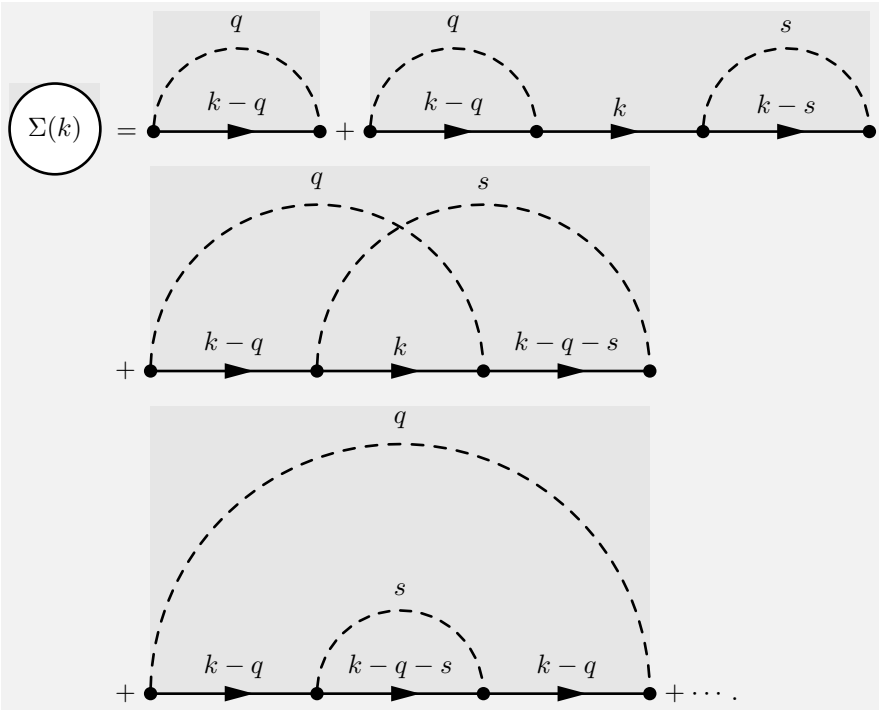

(2.61)

A related quantity is the proper self-energy $\Sigma^*(k)$ which is made up by a subset of the self-energy diagrams. These diagrams are said to be irreducible, meaning that they cannot be split in two by cutting only one propagator, e.g. the first, third and fourth diagram in (2.61). The second diagram in the same expression can be split in half by cutting the electronic propagator with four-momenta k and is then said to be a reducible diagram. With this definition of the proper self-energy, the self-energy is nothing but

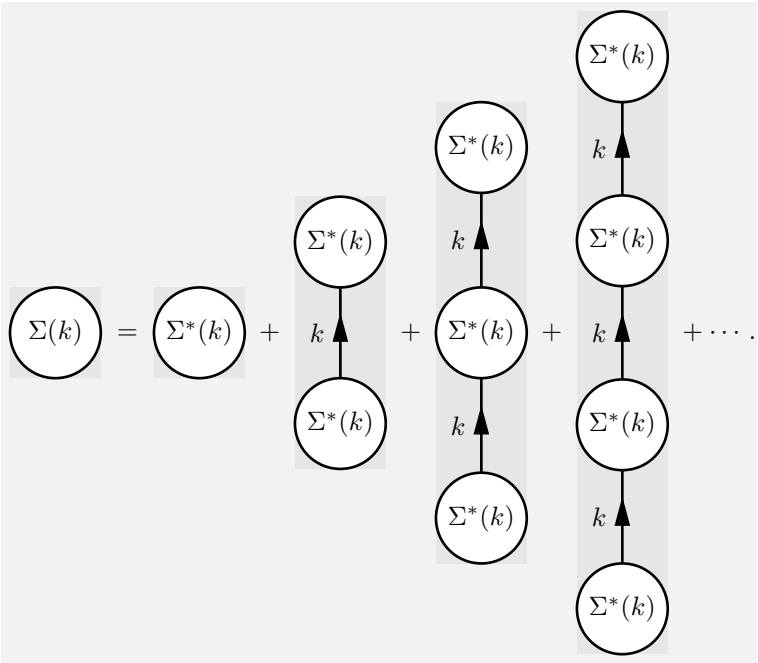

(2.62)

By inserting (2.62) into (2.60), breaking out the factor $\mathcal{G}_0(k)\Sigma^*(k)$ from every diagram but the bare propagator and identifying what is left with $\mathcal{G}(k)$ one obtains a self consistent expression for $\mathcal{G}(k)$ known as Dyson's equation,

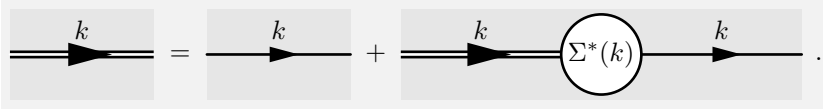

(2.63)

Hence the equation for $\mathcal{G}(k)$ in terms of $\mathcal{G}_0(k)$ and $\Sigma^*(k)$ becomes

$$\mathcal{G}(k) = \frac{1}{\mathcal{G}_0(k)^{-1} - \Sigma^*(k)}\,. \tag{2.64}$$

2.5 Monte Carlo Methods

- Rely on repeated sampling of random numbers to obtain results.

- Use randomness to solve problems which might be deterministic in principle.
- Useful when there is difficult to approach the problem in other way.
- Draw a sequence on numbers from a probability distribution.

2.5.1 Detailed balance and ergodicity

Mention what a Markov process is and what is meant by a stationary distribution for a Markov process

2.5.2 Metropolis-Hastings algorithm

The Metropolis-Hastings algorithm is a Markov chain Monte Carlo method for obtaining a sequence of random samples from a probability distribution for which direct sampling would be difficult. Briefly speaking, this algorithm is able to draw samples from any distribution $P(x)$ given that it is possible to compute the value of a function $f(x)$ which is proportional to the probability density function $\rho(x)$ of the distribution $P(x)$. The Metropolis-Hastings algorithm suggests constructing transition probabilities $P(x|x')$ in order to design a Markov process for which the stationary distribution $\pi(x)$ is chosen to be $P(x)$. By using a Markov process, any random sample being generated is then dependent only on the preceding one.

The starting point to derive the Metropolis-Hastings algorithm is to consider detailed balance between any two states x and x',

$$P(x)\,P(x|x') = P(x')\,P(x'|x)\,, \tag{2.65}$$

Move up to the section above which is about detailed balance.

and then to separate the transitional probabilities into two parts; the proposal $W(x|x')$ and acceptance-rejection $A(x|x')$. Here $W(x|x')$ is the conditional probability distribution of proposing state x' given state x and similarly $A(x|x')$ is the conditional probability distribution of accepting the proposed state x' given x. Expressing the transitional probability as a product of these two parts, i.e. $P(x|x') = W(x|x')\,A(x|x')$, equation (2.65) might be rewritten as

$$\frac{A(x|x')}{A(x'|x)} = \frac{P(x)}{P(x')}\frac{W(x'|x)}{W(x|x')}\,. \tag{2.66}$$

In order to fulfill the condition above, it is common to use the Metropolis choice for the acceptance,

$$A(x|x') = \min\left(1,\, \frac{P(x)}{P(x')}\frac{W(x'|x)}{W(x|x')}\right) = \min\left(1,\, \frac{f(x)}{f(x')}\frac{W(x'|x)}{W(x|x')}\right)\,. \tag{2.67}$$

where the proportionality between the density of P and f has been used in order to reach the last equality. The new state x' is then accepted according to $A(x|x')$.

In practice this is done by sampling a uniform random number a between 0 and 1 and accepting the proposed transition if $A(x|x') > a$, otherwise the transition is rejected. Important to realize here is that if the proposed state x' is rejected, the old state x is then to be thought of as having been sampled yet again in the sequence of states.

- Mention why $A = 1$ is pursued. Better statistics something...

Having performed the algorithm for a while, the state at hand may be considered independent from the initial state. At that point, starting to keep track of how many times a state x is sampled should in the long time limit converge to $\pi(x)$ apart from a normalization factor.

- Mention something about ergodicity being important since it otherwise would be impossible to reach some states.

Chapter 3

Diagrammatic Monte Carlo

Here we shall summarize what this chapter is about

3.1 General idea

"The diagrammatic Monte Carlo (DMC) method [1] is a technique that allows one to simulate quantities specified in terms of convergent diagrammatic sums, i.e., sums of integrals with integrands represented by a diagrammatic structure"

In thermal equilibrium

Diagrammatic Monte Carlo (from here on abbreviated DMC) is a numerical method developed by Prokof'ev et al. [2] in order to calculate quantities $Q(\{y\})$, given in terms of a series of integrals with an ever increasing number of integration variables

$$Q(\{y\}) = \sum_{n=0}^{\infty} \sum_{\xi_n} \int \mathrm{d}x_1 \ldots \mathrm{d}x_n \, D_n(\xi_n, \{y\}, x_1, \ldots, x_n) \,. \tag{3.1}$$

Here $\{y\}$ is a set of external variables and ξ_n indexes the different terms of order n which are given by the function D_n. Terms corresponding to $n = 0$ are understood as being known functions of the external variables. In case of a discrete internal variable x_i, the corresponding integral is exchanged in favor of a sum.

The method is based on the Metropolis-Hastings algorithm which samples terms of the integral series in the $(\xi_n, \{y\}, x_1, \ldots, x_n)$ parameter space. That is, a random walk is preformed between the different integrands in the integral series, as well as between the possible values of the integration variables. In this random walk it is also permissible to include one or more of the external variables. Since the terms at $n = 0$ are known functions it is then possible to calculate the value of Q by keeping track of the frequency by which these terms are sampled, as well as the length of the sequence of sampled terms.

To clarify any ambiguities, the DMC method will next be demonstrated by a few simple examples.

3.1.1 Example 1

In this example the task is to compute $1 + C$, where for convenience it is assumed that $C > 1$ is a constant. The integral series (3.1) will then consist out of two constant zeroth order terms only, making the parameter space discrete with the two possibilities $\xi_0 = 0$ and $\xi_0 = 1$ corresponding to the terms 1 and C respectively. Hence this is probably the simplest possible implementation of DMC and will make for a good first encounter.

The function D_n here play the role of f in the previous section about the MH algorithm.

To follow the recipe of the Metropolis-Hastings algorithm, the function f is defined as being nothing but $D_0(\xi_0)$ from (3.1). By this definition f becomes proportional to the probability density function

$$\rho(x) = \frac{f(x)}{\sum_y f(y)} = \frac{f(x)}{1+C}\,; \quad x \in \{1\,, C\}\,, \tag{3.2}$$

from whose probability distribution function P the sequence of ξ_0's will be drawn. Further more there can be at most four types of transitions between the two states in parameter space. By introducing the corresponding transition probabilities: $P(1|C)$, $P(C|1)$, $P(1|1)$ and $P(C|C)$, the Markov process (is this the correct word?) to be simulated may then be illustrated as in figure (3.1) below.

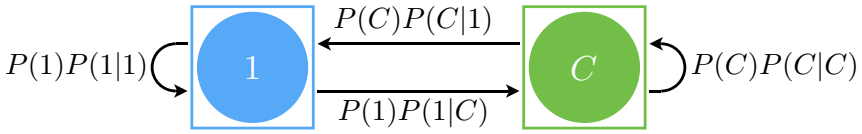

Figure 3.1: Caption this plz!

To simplify matters, the proposal distributions $W(1|C)$, $W(1|1)$, $W(C|1)$ and $W(C|C)$ are all chosen to have the same probability of $1/2$. Then, according to (2.67), the acceptance-rejection ratios will be given by $A(1|1) = A(1|C) = A(C|C) = 1$ and $A(C|1) = 1/C$. By keeping track of how many times $\xi_0 = 0$ appears in the generated sequence, lets say N_0 times, as well as the the total length N of the sequence, it is possible to calculate $1 + C$. This since

$$N_0 \propto \rho(1) \propto 1\,, \quad N - N_0 \propto \rho(C) \propto C \quad \Rightarrow \quad \frac{N_0}{N - N_0} = \frac{1}{C} \tag{3.3}$$

so that

$$1 + C = 1 + \frac{N - N_0}{N_0}\,. \tag{3.4}$$

Include an implementation written in python?

3.1.2 Example 2

In this second example the task is to compute the sum $1 + \int_a^b x \, \mathrm{d}x$.

the only unknown here is the value of the integral. The 1 is solely used for normalization purposes.

Instead of having of having two zeroth order terms as in the first example, there is now a zeroth and first order term. This implies that the parameter space is no longer completely discrete with merely two possible states. Similarly to the first example, the zeroth order term is still represented in parameter space by the state $\xi_0 = 0$. On the other hand, the first order term corresponds to the infinite number of states ($\xi_1 = 0,\, x \in [a,\, b]$). This notation of the states in parameter space is a little cumbersome, however, by assuming $b > a > 1$ it is possible to create a one-to-one mapping which maps $\xi_0 = 0$ and ($\xi_1 = 0,\, x \in [a,\, b]$) onto $x = 1$ and $x \in [a,\, b]$ respectively. Using this notation, a function f is defined by

$$f(x) = \begin{cases} D_0(\xi_0 = 0) = 1\,, & x = 1 \\ D_1(\xi_1 = 0, x) = x\,, & x \in [a,\, b]\,, \end{cases} \tag{3.5}$$

and thus becomes proportional to the probability density

$$\rho(x) = \frac{f(x)}{\sum_y \rho(y)} = \frac{f(x)}{1 + \int_a^b x \, \mathrm{d}x}\,; \quad x \in \{1\} \cup [a,\, b]\,. \tag{3.6}$$

In order to cover the whole parameter space, it is more than sufficient to consider four types of transitions having the transition probabilities $P(1|1)$, $P(1|x)$, $P(x|1)$ and $P(x|x')$. Here it is understood that $x, x' \in [a,\, b]$ and thus corresponds to a state of the first order term. This Markov process might be illustrated as figure 3.2 below.

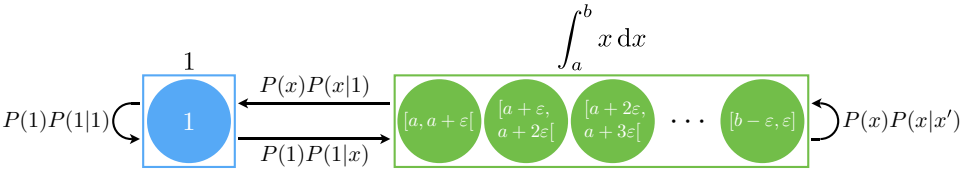

Figure 3.2: Caption this plz!

In order to construct proposal distributions to or from the first order term, it is convenient to introduce the collection of states referred to as $\int$, in which all states $x \in [a,\, b]$. Using this notation, the proposal distributions are chosen to be

$$\begin{aligned} W(1|1) &= \tfrac{1}{2} & W(1|x) &= W(1|\textstyle\int)\, U_{a,b}(x) = \tfrac{1}{2}\tfrac{1}{b-a} \\ W(x|1) &= W(\textstyle\int|1) = \tfrac{1}{2} & W(x|x') &= W(\textstyle\int|\int)\, U_{a,b}(x') = \tfrac{1}{2}\tfrac{1}{b-a}\,. \end{aligned} \tag{3.7}$$

The quantities $W(1|1)$, $W(1|\int)$, $W(\int|1)$ and $W(\int|\int)$ are simply the probability of proposing a state corresponding to a certain term in the integral series and have been set equally probable. The quantity $U_{a,b}(x) = [b-a]^{-1}$ is the uniform probability distribution on the interval $[a, b]$ from which x is sampled. Then, from the proposal distributions follow the acceptance rations

$$\begin{aligned} A(1|1) &= 1 & A(1|x) &= \min\Big(1,\, [b-a]\, x\Big) \\ A(x|1) &= \min\Big(1,\, [b-a]^{-1}\, x^{-1}\Big) & A(x|x') &= \min\Big(1,\, x^{-1}\, x'\Big)\,. \end{aligned} \tag{3.8}$$

By keeping track of the N_0 number of times $x = 1$ appears in the sequence of states and also the length N of the sequence, it follows from (3.3) and (3.4) that

$$1 + \int_a^b x\,\mathrm{d}x = 1 + \frac{N - N_0}{N_0}\,. \tag{3.9}$$

3.1.3 Example 3

In this third and final example, the task is to compute something which is more similar to the actual problem. Hence, the sum to compute is of the form,

$$1 + \int_a^b \mathrm{d}x\, e^{-x} + \int_{a'}^{b'} \mathrm{d}y \int_{a''}^{b''} \mathrm{d}z\, e^{-y-z}\,, \tag{3.10}$$

and consists of a zeroth, first and second order term. By assuming that $b > a > 1$, a similar one-to-one mapping of the states in parameter space as used in the previous example may also be used here. Again the zeroth and first order terms are chosen to be represented by $x = 1$ and $x \in [a, b]$ respectively, whilst the second order term is to be represented by $x = (y, z) \in [a', b'] \times [a'', b'']$. In terms of this parameter x, the function f is defined as

$$f(x) = \begin{cases} D_0(\xi_0 = 0) = 1\,, & x = 1 \\ D_1(\xi_1 = 0, x) = e^{-x}\,, & x \in [a,\, b] \\ D_2(\xi_2 = 0, x) = e^{-y-z}\,, & x \in [a',\, b'] \times [a'',\, b'']\,. \end{cases} \tag{3.11}$$

By normalization a probability density function ρ is obtained whose probability distribution P and seven types of transitions form a Markov process illustrated in figure 3.3.

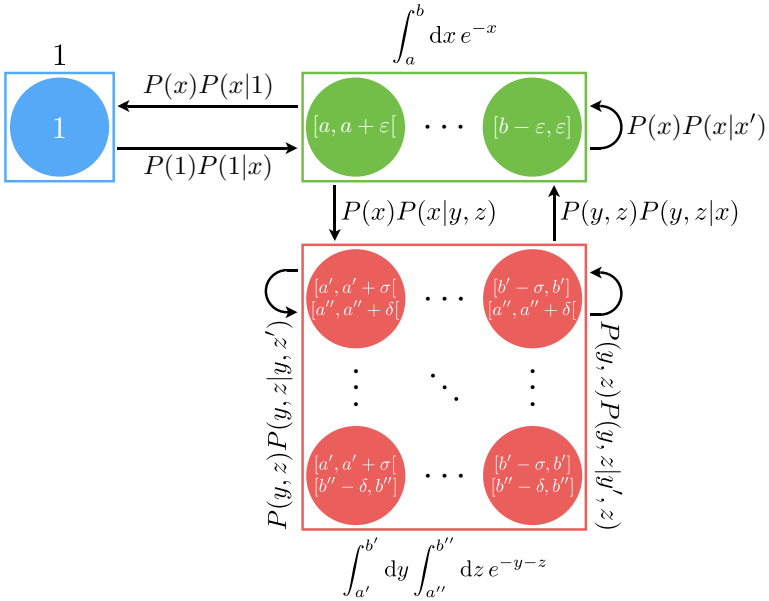

Figure 3.3: Caption this plz!

In order to construct transition probabilities it is convenient to introduce the collection of states $\int$ and $\iint$. These contain all states in parameter space corresponding the first and second order term respectively. The transition probabilities are then chosen as

$$\begin{aligned} W(1|x) &= W(1|\textstyle\int)\, U_{a,b}(x) & W(x|y,z) &= W(\textstyle\int|\iint)\, U_{a',b'}(y)\, U_{a'',b''}(z) \\ W(x|1) &= W(\textstyle\int|1) & W(y,z|y',z) &= W(\iint|\iint)\, W(\iint|y')\, U_{a',b'}(y') \\ W(y,z|x) &= W(\iint|\textstyle\int)\, U_{a,b}(x) & W(y,z|y,z') &= W(\iint|\iint)\; W(\iint|z')\, U_{a'',b''}(z') \\ W(x|x') &= W(\textstyle\int|\int)\, U_{a,b}(x')\,, \end{aligned} \tag{3.12}$$

where

$$\begin{aligned} W(1|\textstyle\int) &= 1 \\ W(\textstyle\int|1) = W(\int|\int) &= W(\int|\iint) = \tfrac{1}{3} \\ W(\iint|\int) = W(\iint|\iint) &= W(\iint|y') = W(\iint|z') = \tfrac{1}{2}\,. \end{aligned} \tag{3.13}$$

The discrete proposal distributions $W(\iint|y')$ and $W(\iint|z')$ correspond to choosing to update either the y or the z part of the state x. Having all of this information

it is then trivial to calculate the acceptance ratios, which become

$$\begin{aligned}
W(1|x) &= \min\Big(1,\ \tfrac{1}{3}[b-a]\, e^{-x}\Big)\\
W(x|1) &= \min\Big(1,\ 3\,[b-a]^{-1}\, e^{x}\Big)\\
W(x|x') &= \min\Big(1,\ e^{x-x'}\Big)\\
W(x|y,z) &= \min\Big(1,\ \tfrac{2}{3}[b'-a'][b''-a'']\,[b-a]^{-1}\, e^{x-y-z}\Big)\\
W(y,z|x) &= \min\Big(1,\ \tfrac{3}{2}[b'-a']^{-1}[b''-a'']^{-1}[b-a]\, e^{y+z-x}\Big)\\
W(y,z|y',z) &= \min\Big(1,\ e^{y-y'}\Big)\\
W(y,z|y,z') &= \min\Big(1,\ e^{z-z'}\Big)\,.
\end{aligned} \tag{3.14}$$

By defining N_0 and N in accordance to what was done in the previous example, the value of the sum is obtained by

$$1+\int_a^b \mathrm{d}x\, e^{-x}+\int_{a'}^{b'}\mathrm{d}y\int_{a''}^{b''}\mathrm{d}z\, e^{-y-z}=1+\frac{N-N_0}{N_0}\,. \tag{3.15}$$

3.2 Implementation

The task at hand is now to implement the DMC method in order to calculate the electronic single-particle Green's function $\mathcal{G}(\alpha,\mu,\mathbf{p},\tau)$. The integral series (3.1) will then be nothing but the diagrammatic series (2.58), with the external parameters $\{y\}=\{\alpha,\mu,\mathbf{p},\tau\}$. The integration variables x_i's must therefore correspond to the internal imaginary-times and momenta, where the internal momenta are chosen to be those of the phonon propagators. By then representing the internal momenta in spherical coordinates $\mathbf{q}=(q\sin\theta\cos\varphi, q\sin\theta\sin\varphi, q\cos\theta)$, the momentum integrals should be replaced according to

$$\int\frac{\mathrm{d}^3q}{(2\pi)^3}\to\int_{q=0}^{\infty}\int_{\theta=0}^{\pi}\int_{\varphi=0}^{2\pi}\frac{q^2\sin\theta\,\mathrm{d}q\,\mathrm{d}\theta\,\mathrm{d}\varphi}{(2\pi)^3}\,. \tag{3.16}$$

The beauty of this is realized when recalling that each phonon brings with it a factor $V(q)^2\propto q^{-2}$, whose momentum dependence exactly cancel with that of the integral. For example, the expression corresponding the first order diagram then becomes

$$-\int_0^{\tau}\mathrm{d}\tau_2\int_0^{\tau_2}\mathrm{d}\tau_1\int_0^{\infty}\mathrm{d}q\int_0^{\pi}\mathrm{d}\theta\int_0^{2\pi}\mathrm{d}\varphi\,\mathcal{G}_0(\mathbf{p},\tau_1)\mathcal{G}_0(\mathbf{p}-\mathbf{q},\tau_2-\tau_1)\tilde{\mathcal{D}}_0(\mathbf{q},\tau_2-\tau_1)\mathcal{G}_0(\mathbf{p},\tau-\tau_2)\,, \tag{3.17}$$

where $\tilde{\mathcal{D}}_0(\mathbf{q},\tau)$ is a phonon propagator which has absorbed the factor $q^2 \sin\theta\,(2\pi)^{-3}$ originating from the integral, the interaction potential $V(q)^2$ along with the factor -1 from the Feynman rules. Thus

$$\tilde{\mathcal{D}}_0(\mathbf{q},\tau) = \frac{2\sqrt{2}\pi\alpha}{(2\pi)^3}\sin\theta\,\exp\{-\tau\} \tag{3.18}$$

which is a quantity always larger than or equal to zero. The integrand of each and every integral in the integral series will be entirely made up out of $\mathcal{G}_0$'s and $\tilde{\mathcal{D}}_0$'s which implies that every contribution to $\mathcal{G}$ is a positive contribution. This will simplify the DMC implementation since it wont be necessary to calculate what sign each sampled parameter space state comes with.

The external parameters $\mathbf{p}$ and τ will be the only ones allowed to change during the Markov process. Including α and/or μ would cause the parameter space to increase and the statistics to be spread out. Thus more computation time would be needed to calculate quantities to the same level of certainty as having α and μ fixed.

The value of the propagator $\mathcal{G}$ will be computed at the discrete set of points $\mathbf{p}_i = \Delta p(0.5+i)\,\hat{\mathbf{e}}_z$ and $\tau_j = \Delta\tau(0.5+j)$ where $i = 0, 1, 2, \ldots, N-1$, $j = 0, 1, 2, \ldots, M-1$ and the resolution is chosen in terms of Δp and $\Delta\tau$. To calculate $\mathcal{G}(\mathbf{p}_i,\tau_j) = \mathcal{G}_{i,j}$, both a bin N_0 and a two dimensional histogram N are used, even though $\mathbf{p}$ and τ will be continuous variables. Thus the bin $N_{i,j}$ of the histogram will be covering the range $p \in [p_i - \Delta p/2,\, p_i + \Delta p/2]$ and $\tau \in [\tau_j - \Delta\tau/2,\, \tau_j + \Delta\tau/2]$ of the external parameter values. The value of every bin in the histogram along with N_0 are initially put to zero. Then, each time a parameter space state is sampled, it will be checked wether or not this state belongs to the zeroth order term $\mathcal{G}_0(\mathbf{p},\tau)$. If this is the case, the value of N_0 is increased by 1, if not, the bin in the histogram according to the external parameters is increased by 1. By doing this, the quantities N_0 and $N_{i,j}$ can be shown to be proportional to

$$\begin{aligned} N_0 &\propto \int_0^{N\Delta p} \mathrm{d}p \int_0^{M\Delta p} \mathrm{d}\tau\, \mathcal{G}_0(\mathbf{p},\tau) \\ &= \Delta p\,\Delta\tau \sum_{k,l} \mathcal{G}_0(\mathbf{p}_k,\tau_l) + \mathcal{O}\left([\Delta p]^3 + [\Delta\tau]^3\right) \end{aligned} \tag{3.19}$$

and

$$\begin{aligned} N_{i,j} &\propto \int_{p_{i-0.5}}^{p_{i+0.5}} \mathrm{d}p \int_{\tau_{j-0.5}}^{\tau_{j+0.5}} \mathrm{d}\tau\, [\mathcal{G}(\mathbf{p},\tau) - \mathcal{G}_0(\mathbf{p},\tau)] \\ &= \Delta p\,\Delta\tau\, [\mathcal{G}(\mathbf{p}_i,\tau_j) - \mathcal{G}_0(\mathbf{p}_i,\tau_j)] + \mathcal{O}\left([\Delta p]^3 + [\Delta\tau]^3\right) \end{aligned} \tag{3.20}$$

respectively. Omitting the errors due to discretization, the interacting electronic propagator is then found to be

$$\mathcal{G}(\mathbf{p}_i, \tau_j) = \mathcal{G}_0(\mathbf{p}_i, \tau_j) + N_{i,j} \frac{\sum_{k,l} \mathcal{G}_0(\mathbf{p}_k, \tau_l)}{N_0} \,. \tag{3.21}$$

On the other hand, if the external momentum where to be held fixed at $\mathbf{p}_0$, the value of $\mathcal{G}$ at the set of imaginary-times $\{\tau_j\}$ would similarly become

$$\mathcal{G}(\mathbf{p}_0, \tau_j) = \mathcal{G}_0(\mathbf{p}_0, \tau_j) + N_j \frac{\sum_{l} \mathcal{G}_0(\mathbf{p}_0, \tau_l)}{N_0} \,. \tag{3.22}$$

Here the histogram N has only one dimension corresponding to the different τ_j.

- introduce $\tau_{\max}$ and $p_{\max}$.
- Quickly mention the code implementation. momenta belongs to lines, time to nodes. Nodes instead of vertices in order to keep things general (when sampling $\Sigma*$)

3.3 Bare scheme update procedures for $\mathcal{G}$

What remains to be discussed is how the sampling of states in parameter space occurs. As the name Diagrammatic Monte Carlo suggest, the diagrammatic representation of the integral series will be used. That is, the functions D_n in the integral series (3.1) is to be though of as a Feynman diagram (without the integrals). The random walk, which is used to simulate the Markov process, will thus be in terms of such diagrams. It is then important that each and every such diagram must be possible to reach in order to cover all of parameter space and thus maintaining ergodicity. To make sure that this actually is the case, a set of update procedures [2] have been constructed.

Change of diagram length in time, type 1

Figure 3.4: The only affected parameter is the highlighted imaginary-time of the end point node.

This update procedure merely changes the external imaginary-time parameter τ, which is nothing but the diagram length in time. In the first update type this is

achieved by altering the time of the end point node in the diagram, i.e. $\tau \to \tau'$, as illustrated in figure 3.4. The only affected quantity of such an update will be the value of the very last $\mathcal{G}_0$ in the diagram so that

$$\frac{D_n(\tau')}{D_n(\tau)} = \frac{\mathcal{G}_0(\mathbf{p}, \tau' - \tau_{2n})}{\mathcal{G}_0(\mathbf{p}, \tau - \tau_{2n})} = \frac{\exp\left\{-\left(\frac{p^2}{2} - \mu\right)\tau'\right\}}{\exp\left\{-\left(\frac{p^2}{2} - \mu\right)\tau\right\}} \tag{3.23}$$

Now consider an exponential distribution on the interval $[\tau_{2n}, \tau_{\max}]$ with rate parameter $\lambda = p^2/2 - \mu$ of which the density is

$$\rho(\tau) = \frac{\lambda\, e^{-\lambda(\tau - \tau_{2n})}}{1 - e^{-\lambda(\tau_{\max} - \tau_{2n})}}\,. \tag{3.24}$$

By sampling τ' from such a distribution, the ratio $W(\tau'|\tau)/W(\tau|\tau')$ will be the inverse of D'_n/D_n. Hence the acceptance ratio $A(\tau|\tau')$ of this update procedure becomes 1, and any proposed τ' is always be accepted.

Change of diagram length in time, type 2

- Mention something about the probability of choosing a node on random will cancel is chosen uniformly. Tell the reader that this is also the case for all other updates procedures as long as nothing else is said.

Figure 3.5: The highlighted τ's are the parameters affected by this update.

This update procedure also changes the external imaginary-time parameter, although it does so in a slightly different by letting any $\mathcal{G}_0$ in the diagram be lengthen or shortened in time, not just the last one. This is achieved by randomly picking any but the leading node in the diagram to assign a new imaginary-time τ'_k from the interval $[\tau_{k-1}, \tau_{\max} - (\tau - \tau_k)]$. In order to only modify the length of the electronic propagator just in front of the chosen node, every node proceeding this node must clearly have the difference $\tau'_k - \tau_k$ added to its time. This is illustrated in figure 3.5.

This update does not merely affect the one $\mathcal{G}_0$, but phonon propagators with start and end points on different sides of the chosen node would also have their

length modified by the difference $\tau'_k - \tau_k$. If there are m such phonons, the quota of the diagram values become

$$\begin{aligned}\frac{D_n(\tau')}{D_n(\tau)} &= \frac{\mathcal{G}_0(\mathbf{p}, \tau_k - \tau_{k-1}) \prod_{i=0}^{m-1} \tilde{\mathcal{D}}_0(\mathbf{q}_i, \Delta\tau_i)}{\mathcal{G}_0(\mathbf{p}, \tau'_k - \tau_{k-1}) \prod_{j=0}^{m-1} \tilde{\mathcal{D}}_0(\mathbf{q}_j, \Delta\tau_j + [\tau'_k - \tau_k])} \\ &= \frac{\exp\left\{-\left(\frac{p^2}{2} - \mu + m\right)\tau'_k\right\}}{\exp\left\{-\left(\frac{p^2}{2} - \mu + m\right)\tau_k\right\}},\end{aligned} \tag{3.25}$$

where $\Delta\tau_i$ is the length in time of the ith phonon propagator. By sampling the τ'_k from an exponential distribution with rate parameter $\lambda = p^2/2 - \mu + m$, the acceptance ration for this update procedure also becomes unity.

This second version of the change of diagram length update procedure is more complex than the first one, and may therefore be chosen less often. In a worst case scenario the complexity scales as $\mathcal{O}(2n)$, due to figuring out the number of phonons m just discussed. Only one of the procedures changing the length of the diagram would be sufficient, but having an over complete set of update procedures is necessarily not something negative and could potentially enhance the statistics.

Change of external momentum

Figure 3.6: This update procedure changes the momentum of every $\mathcal{G}_0$ in the diagram by the external momentum difference $\mathbf{p}' - \mathbf{p}$. Surely it must be the case that $\mathbf{p}_0 = \mathbf{p}_{2n} = \mathbf{p}$ and the same is of course true in primed case as well.

Since there is no preferred direction of the Hamiltonian (2.49), the Green's function $\mathcal{G}$ becomes dependent merely upon the magnitude of the external momentum $\mathbf{p}$. (this is supposed to have been discussed at an earlier point!) This update procedure is thus constructed to keep the direction constant while changing only the magnitude $p \to p'$. In order to satisfy momentum conservation at each vertex, the $\mathcal{G}_0$'s are chosen to absorb the external momentum difference $\mathbf{p}' - \mathbf{p}$ leaving the value of

the $\tilde{\mathcal{D}}_0$'s the same. This is illustrated in figure 3.6. The ratio of the diagram value after to before such an update then becomes

$$\begin{aligned}\frac{D_n(\mathbf{p}')}{D'_n(\mathbf{p})} &= \frac{\prod_{i=0}^{2n} \mathcal{G}_0(\mathbf{p}'_i, \tau_{i+1} - \tau_i)}{\prod_{j=0}^{2n} \mathcal{G}_0(\mathbf{p}_j, \tau_{j+1} - \tau_j)} \\ &= \exp\left\{-\frac{1}{2}\sum_{i=0}^{2n}\left(\left[\mathbf{p}_i + (\mathbf{p}' - \mathbf{p})\right]^2 - p_i^2\right)(\tau_{i+1} - \tau_i)\right\} \\ &= \exp\left\{-\frac{\tau}{2}\left([p' - p]^2 + 2\langle\mathbf{p}\rangle_{0,2n} \cdot [\mathbf{p}' - \mathbf{p}]\right)\right\}\end{aligned} \tag{3.26}$$

where the mean electronic momentum is defined as

$$\langle\mathbf{p}\rangle_{k,l} \equiv \sum_{i=k}^{l} \frac{\tau_{i+1} - \tau_i}{\tau}\,\mathbf{p}_i\,. \tag{3.27}$$

- Introduce $p_{\min}$ earlier in the thesis

By sampling $p' \in [p_{\min}, p_{\max}]$ using a truncated half-normal distribution whose corresponding normal distribution would have the standard deviation $\sigma = 1/\sqrt{\tau}$, the fraction of the proposal distributions take the value

$$\frac{W(\mathbf{p}'|\mathbf{p})}{W(\mathbf{p}|\mathbf{p}')} = \exp\left\{-\frac{\tau}{2}(p^2 - p'^2)\right\} \tag{3.28}$$

so that the acceptance ratio is found to be

$$\begin{aligned}A(p|p') &= \min\Big(1,\, \exp\left\{-(\mathbf{p}' - \mathbf{p}) \cdot (\langle\mathbf{p}\rangle_{0,2n} - \mathbf{p})\,\tau\right\}\Big) \\ &= \min\Big(1,\, \exp\left\{-(p' - p)\,(\langle p_z\rangle_{0,2n} - p)\,\tau\right\}\Big)\,.\end{aligned} \tag{3.29}$$

In the final equality the vectors has ben represented in a Cartesian coordinate system with the z-axis parallel to the external momentum. On average $\langle p_z\rangle_{0,2n}$ should not differ to much from p, implying that both the exponential and the acceptance ration should be close to unity most of the time. This of course being the reason why the update procedure is constructed the way it is.

Perhaps $\langle p_z\rangle_{0,2n} = p$ on average?

Change of transferred momentum magnitude

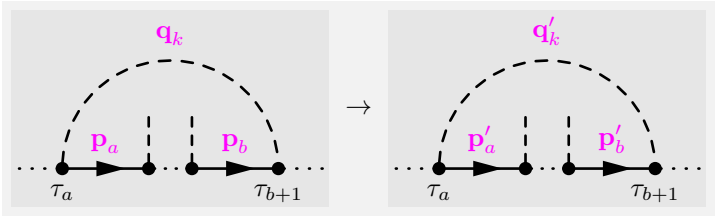

Figure 3.7: The momentum transferred via an internal phonon propagator is updated. In order obey momentum conservation at every vertex, electronic propagators beneath the phonon arc absorb the momentum difference.

This update procedure is designed to be very similar to that of the external momentum. However, the main difference of course being that the magnitude of momentum transferred via a phonon propagator is updated rather than the external momentum. In order to achieve this, a $\tilde{\mathcal{D}}_0$ is randomly picked and has a new momentum magnitude assigned to it $q_k \to q'_k$ while keeping the direction fixed. In order to conserve momentum at the two vertices connected to the phonon propagator, the $\mathcal{G}_0$'s located beneath the phonon arc should absorb the momentum difference $\mathbf{q}_k - \mathbf{q}'_k$. This is illustrated in figure 3.7. Since the $\tilde{\mathcal{D}}(\mathbf{q}, \tau)$'s does not depend on the magnitude $q = |\mathbf{q}|$, the ratio of diagram values become

$$\begin{aligned}\frac{D_n(\mathbf{q}'_k)}{D_n(\mathbf{q}_k)} &= \frac{\prod_{i=a}^{b} \mathcal{G}_0(\mathbf{p}'_i, \tau_{i+1} - \tau_i)}{\prod_{j=a}^{b} \mathcal{G}_0(\mathbf{p}_j, \tau_{j+1} - \tau_j)} \\ &= \exp\left\{ -\frac{1}{2} \sum_{i=a}^{b} \left(\left[\mathbf{p}_i + (\mathbf{q}_k - \mathbf{q}'_k)\right]^2 - p_i^2 \right) (\tau_{i+1} - \tau_i) \right\} \\ &= \exp\left\{ -\frac{\tau_{b+1} - \tau_a}{2} \left([q_k - q'_k]^2 + 2\langle \mathbf{p} \rangle_{a,b} \cdot [\mathbf{q}_k - \mathbf{q}'_k] \right) \right\},\end{aligned} \tag{3.30}$$

which indeed is similar to (3.26). Following in the footsteps of the previous update procedure, $q'_k \in [0, \infty[$ is sampled from a half-normal distribution whose corresponding normal distribution would have the standard deviation $\sigma = 1/\sqrt{\tau_{b+1} - \tau_a}$. The acceptance ration is then found to be,

$$A(\mathbf{q}_k | \mathbf{q}'_k) = \min\Big(1,\, \exp\left\{ -(\mathbf{q}_k - \mathbf{q}'_k) \cdot (\langle \mathbf{p} \rangle_{a,b} + \mathbf{q}_k) \left[\tau_{b+1} - \tau_a\right] \right\} \Big). \tag{3.31}$$

It is reasonable to assume that on average, $\langle \mathbf{p} \rangle_{a,b} + \mathbf{q}_k$ does not differ too much from the external momentum $\mathbf{p}$. Hence this update procedure should have an acceptance

ration close to unity at low external momenta whilst performing worse at higher external momenta.

Change of transferred momentum direction

This update procedure changes the direction $(\theta_k,\, \varphi_k) \to (\theta'_k,\, \varphi'_k)$ of the momentum transferred via a phonon propagator. As in the previous update procedure, the electronic propagators below the phonon arc absorb the momentum difference $\mathbf{q}_k - \mathbf{q}'_k$ which is illustrated in figure 3.7. This time, since $\tilde{\mathcal{D}} \propto \sin\theta$ the ratio of the diagram values becomes slightly different

$$\begin{aligned}\frac{D_n(\mathbf{q}'_k)}{D_n(\mathbf{q}_k)} &= \frac{\sin\theta'_k}{\sin\theta_k}\frac{\prod_{i=a}^{b}\mathcal{G}_0(\mathbf{p}'_i, \tau_{i+1}-\tau_i)}{\prod_{j=a}^{b}\mathcal{G}_0(\mathbf{p}_j, \tau_{j+1}-\tau_j)} \\ &= \frac{\sin\theta'_k}{\sin\theta_k}\exp\left\{-\frac{\tau_{b+1}-\tau_a}{2}\left([\mathbf{q}_k-\mathbf{q}'_k]^2 + 2\langle\mathbf{p}\rangle_{a,b}\cdot[\mathbf{q}_k-\mathbf{q}'_k]\right)\right\}.\end{aligned} \tag{3.32}$$

By sampling the azimuthal angle uniformly on the interval $\varphi'_k \in [0,\, 2\pi]$, and the polar angle $\theta'_k \in [0,\, \pi]$ from a probability distribution whose density $\rho(\theta'_k) = \frac{1}{2}\sin\theta'_k$, one obtains the acceptance ratio

$$A(\mathbf{q}_k|\mathbf{q}'_k) = \min\left(1,\, \exp\left\{-\frac{\tau_{b+1}-\tau_a}{2}\left([\mathbf{q}_k-\mathbf{q}'_k]^2 + 2\langle\mathbf{p}\rangle_{a,b}\cdot[\mathbf{q}_k-\mathbf{q}'_k]\right)\right\}\right). \tag{3.33}$$

Vertex shift in time

Figure 3.8: The imaginary-time of internal node k is updated.

This update procedure changes the imaginary-time $\tau_k \to \tau'_k$ of a randomly chosen internal node whilst keeping the chronological ordering, i.e $\tau_{k-1} < \tau'_k < \tau_{k+1}$. The procedure is illustrated in figure 3.8, and as can be seen, it does only affect the three propagators connected to the node so that

$$\begin{aligned}\frac{D_n(\tau'_k)}{D_n(\tau_k)} &= \frac{\mathcal{G}_0(\mathbf{p}_{k-1}, \tau'_k-\tau_{k_1})\,\mathcal{G}_0(\mathbf{p}_k, \tau_{k+1}-\tau'_k)\,\tilde{\mathcal{D}}_0(\mathbf{q}_k, \pm(\tau_l-\tau'_k))}{\mathcal{G}_0(\mathbf{p}_{k-1}, \tau'_k-\tau_{k_1})\,\mathcal{G}_0(\mathbf{p}_k, \tau_{k+1}-\tau_k)\,\tilde{\mathcal{D}}_0(\mathbf{q}_k, \pm(\tau_l-\tau_k))} \\ &= \exp\left\{-\left[\frac{p_{k-1}^2}{2} - \frac{p_k^2}{2} \mp 1\right](\tau'-\tau)\right\}.\end{aligned} \tag{3.34}$$

Here the upper sign is used if $\tau_l > \tau_k$, meaning that the phonon propagator is leaving to node l from node k. If instead $\tau_l < \tau_k$, the lower sign should be used and the situation becomes the opposite. By sampling τ_k' from the interval $[\tau_{k-1}, \tau_{k+1}]$ using an exponential distribution with rate parameter $\lambda = p_{k-1}^2/2 - p_k^2/2 \mp 1$, the acceptance ration becomes unity.

Change of diagram structure

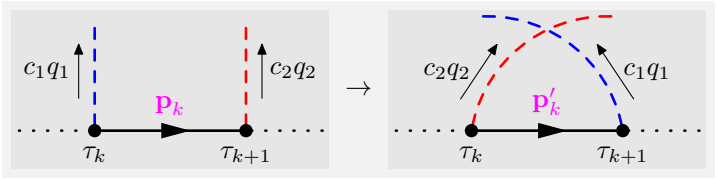

Figure 3.9: The diagram structure is modified by interchanging the phonon propagators connected to two neighboring nodes. Bold face: $\mathbf{q}_1$ and $\mathbf{q}_2$

This update procedure, as illustrated in figure 3.9, interchange the two phonon propagators connected to a pair of randomly selected neighboring nodes. In order to conserve momentum, the $\mathcal{G}_0$ connected to both of the selected nodes must absorb the difference $\mathbf{p}_k' - \mathbf{p}_k = c_1\mathbf{q}_1 - c_2\mathbf{q}_2$. Here the c_i tells whether the propagator is propagating towards any of the two nodes ($c_i = -1$) or if it is propagating away from any of the two nodes ($c_i = 1$). The ratio of the diagram value prior to and after the update then becomes

$$\begin{aligned}\frac{D_n(\xi_n')}{D_n(\xi_n)} &= \frac{\mathcal{D}_0(\mathbf{q}_1, c_1[\tau_i - \tau_{k+1}])\,\mathcal{D}_0(\mathbf{q}_2, c_2[\tau_j - \tau_k])\,\mathcal{G}_0(\mathbf{p}_k', \tau_{k+1} - \tau_k)}{\mathcal{D}_0(\mathbf{q}_1, c_1[\tau_i - \tau_k])\,\mathcal{D}_0(\mathbf{q}_2, c_2[\tau_j - \tau_{k+1}])\,\mathcal{G}_0(\mathbf{p}_k, \tau_{k+1} - \tau_k)} \\ &= \exp\left\{-\left[\frac{(\mathbf{p}_k + c_1\mathbf{q}_1 - c_2\mathbf{q}_2)^2}{2} - \frac{p_k^2}{2} - c_1 + c_2\right](\tau_{k+1} - \tau_k)\right\}.\end{aligned} \tag{3.35}$$

Other than the pair of nodes to be picked, there are no parameters to be sampled in order to change the diagram structure in this way. Thus $W(\xi_n|\xi_n') = W(\xi_n'|\xi_n)$ and the update procedure should be accepted according to

$$A(\xi_n|\xi_n') = \min\left(1, \frac{D_n(\xi_n')}{D_n(\xi_n)}\right). \tag{3.36}$$

Change of digram order

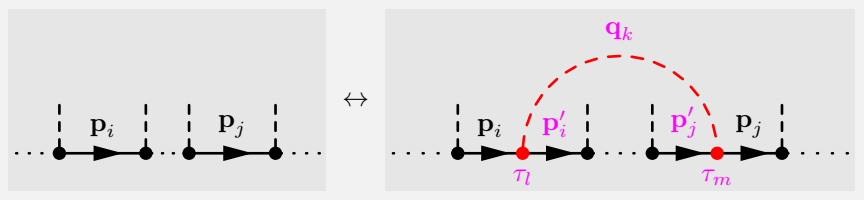

Figure 3.10: An illustration of the change of diagram order procedure.

This final update procedure which is illustrated in figure 3.10, is the only one which changes the order of the diagram at hand. To increase the diagram order, an electronic propagator $\mathcal{G}_{0,i}$ is selected on random and then split at a time τ_l, which is sampled uniformly on the interval $[\tau_i, \tau_{i+1}]$. After this, another imaginary time τ_m is sampled on the interval $\tau_m \in [\tau_l, \tau]$ using an exponential distribution with a rate parameter $\lambda = 1$. The $\mathcal{G}_{0,j}$ which happen to occupy the imaginary-time τ_m is split in twice at that point as well. For each of the two times τ_l and τ_m, a node is inserted so that the loose ends of the $\mathcal{G}_0$'s have something to connect to. The two newly introduced nodes are then further connected to a new phonon propagator $\tilde{\mathcal{D}}_0$, for which the momentum $\mathbf{q}_k$ is sampled according to the *change of transferred momentum* procedures introduced earlier. In order to obey momentum conservation at each node, the $\mathcal{G}_0$'s under the newly added phonon arc have their momentum subtracted by $\mathbf{q}_k$. In this way, the probability distribution of increasing the diagram order becomes

$$W(n|n+1) = P_{\mathrm{R}}(n)\,\frac{1}{2n+1}\,\frac{1}{\tau_{i+1}-\tau_i}\,\frac{e^{-(\tau_m-\tau_l)}}{1-e^{-(\tau-\tau_l)}}\,\frac{\sin\theta_k}{2}\,\frac{1}{2\pi} \times \sqrt{\frac{2(\tau_m-\tau_l)}{\pi}}\exp\left\{-\frac{q_k^2}{2}(\tau_m-\tau_l)\right\}. \tag{3.37}$$

Here $P_{\mathrm{R}}(n)$ is the probability of choosing to raise the diagram order once having selected the *change of diagram order* procedure. Of course the corresponding probability of choosing to lower the diagram order is then nothing but $1-P_{\mathrm{R}}(n)$. Further

more, the ratio of the diagram value prior to and after the update is realized to be

$$\begin{aligned}\frac{D_{n+1}}{D_n} &= \tilde{\mathcal{D}}_0(\mathbf{q}_k, \tau_m - \tau_l) \frac{\prod_{i=l}^{m-1} \mathcal{G}_0(\mathbf{p}_i - \mathbf{q}_k, \tau_{i+1} - \tau_i)}{\prod_{i=l}^{m-1} \mathcal{G}_0(\mathbf{p}_i, \tau_{i+1} - \tau_i)} \\ &= \frac{2\sqrt{2}\pi\alpha}{(2\pi)^3} \sin\theta_k \exp\left\{ -\left[\frac{q_k^2}{2} + 1 - \langle \mathbf{p} \rangle_{l,m-1} \cdot \mathbf{q}_k \right] (\tau_m - \tau_l) \right\} .\end{aligned} \tag{3.38}$$

The procedure of lowering the diagram order is much more simplistic; it is only necessary to randomly pick a $\tilde{\mathcal{D}}$ which is to be removed. Hence $W(n+1|n) = (1 - P_{\mathrm{R}}(n+1))\,[n+1]^{-1}$, and by introducing the quantity

$$\begin{aligned}R(n|n+1) &= \frac{D_{n+1}}{D_n} \frac{W(n+1|n)}{W(n|n+1)} \\ &= \frac{1 - P_{\mathrm{R}}(n+1)}{P_{\mathrm{R}}(n)} \frac{\alpha}{\sqrt{\pi}} \frac{2n+1}{n+1} \frac{\tau_{i+1} - \tau_i}{\sqrt{\tau_m - \tau_l}} \\ &\times \left[1 - e^{-(\tau - \tau_l)} \right] \exp\left\{ [\langle \mathbf{p} \rangle_{l,m-1} \cdot \mathbf{q}_k](\tau_m - \tau_l) \right\}\end{aligned} \tag{3.39}$$

the acceptance ratios may be expressed as

$$A(n|n+1) = \min\left(1,\, R(n|n+1)\right) , \quad A(n+1|n) = \min\left(1,\, 1/R(n|n+1)\right) . \tag{3.40}$$

By requiring that

$$\frac{1 - P_{\mathrm{R}}(n+1)}{P_{\mathrm{R}}(n)} = \frac{\sqrt{\pi}}{2\alpha} \quad \Rightarrow \quad P_{\mathrm{R}}(n) = P_{\mathrm{R}} = \left[1 + \frac{\sqrt{\pi}}{2\alpha} \right]^{-1} \tag{3.41}$$

these acceptance ratios become independent of the coupling constant α and less dependent of the diagram order n

Clearly it should not be possible to lower the diagram order any further than $n = 0$. Also, one could think of implementing a maximum order $n_{\max}$ for which the diagram order should not be able to rise above. To achieve this, it is extremely important not to set $P_{\mathrm{R}} = 1$ and $P_{\mathrm{R}} = 0$ at $n = 0$ and $n = n_{\max}$ respectively, since this would ruin the detailed balance. Rather one should approach this by simply refusing such an update. For example, if the procedure to increase the diagram order happen to be chosen when $n = n_{\max}$, it should be refused and a new update procedure chosen instead.

- Check the acceptance ratio!

3.3.1 Results

- Result should be independent on weight of each update function

Here follow some results obtained when simulating $\mathcal{G}$ using the bare scheme update procedures described above. The external momentum $\mathbf{p}$ has been fixed during these simulations in order to not spread the statistics out over external parameters for which the data is not shown.

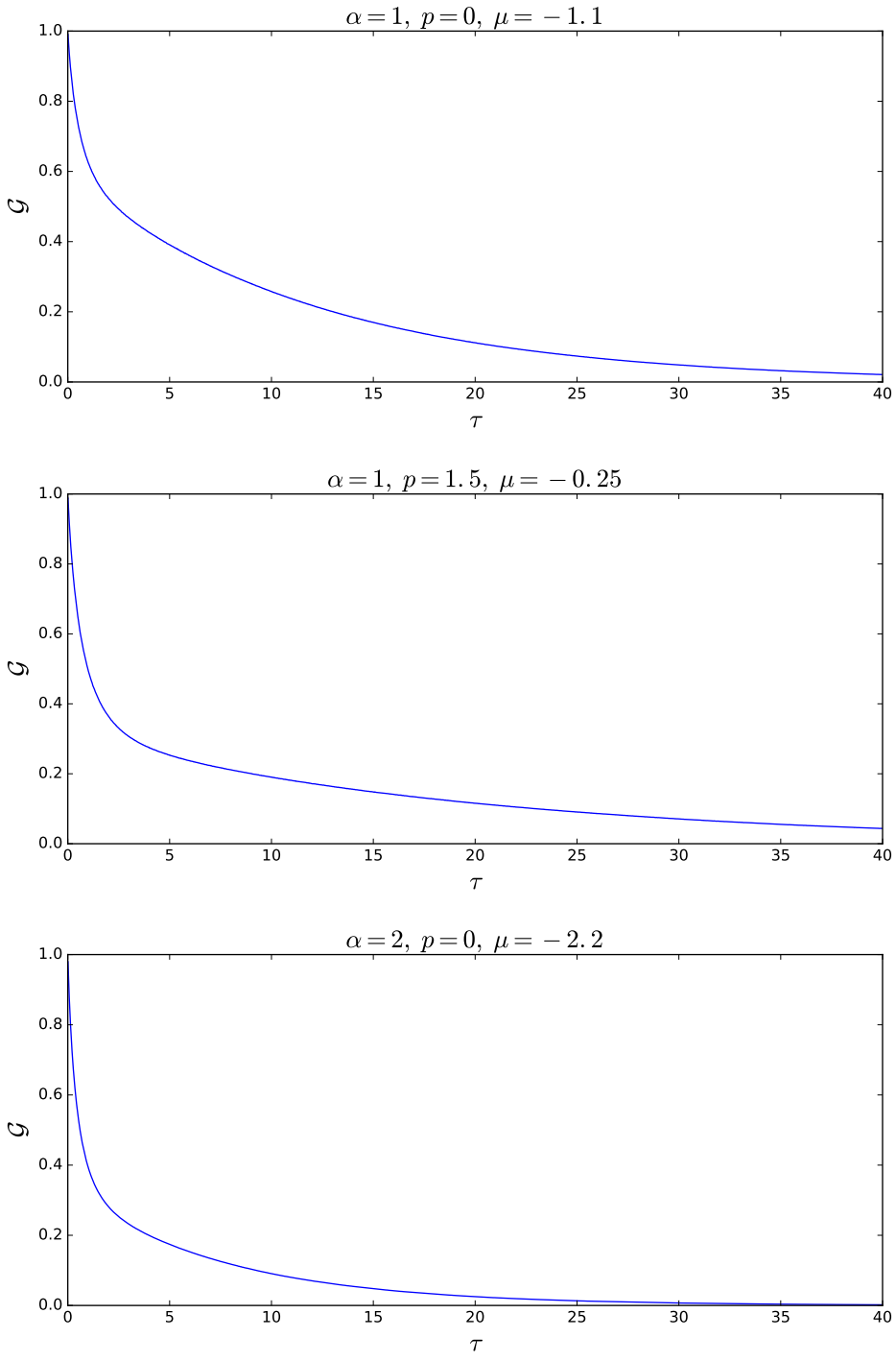

Figure 3.11: The acquired value of $\mathcal{G}(p = 0, \tau)$ after 80 minutes of core time. Here $\tau_{max} = 40$ and $\Delta\tau = 0.02$ has been used.

τ	$\mathcal{G}(0,1,-1.1)$	$\mathcal{G}(1.5,1,-0.25)$	$\mathcal{G}(0,2,-2.2)$
0.01	0.9906	0.9881	0.9797
1.01	0.6242	0.4938	0.3922
2.01	0.5225	0.3631	0.2808
3.01	0.4673	0.3066	0.2314
4.01	0.4259	0.2745	0.1993
5.01	0.3907	0.2528	0.1738
6.01	0.359	0.2365	0.1524
7.01	0.3301	0.223	0.1339
8.01	0.3041	0.2113	0.1176
9.01	0.2797	0.2003	0.1031
10.01	0.2573	0.1902	0.09057
11.01	0.2374	0.1806	0.07967
12.01	0.2175	0.1715	0.07009
13.01	0.2003	0.1635	0.0617
14.01	0.1844	0.1552	0.05428
15.01	0.1695	0.1476	0.04763
16.01	0.156	0.1409	0.04189
17.01	0.1436	0.1341	0.03696
18.01	0.1319	0.1276	0.03243
19.01	0.1213	0.1216	0.02866
20.01	0.1116	0.1157	0.02498
21.01	0.1025	0.1103	0.02211
22.01	0.09434	0.1051	0.01937
23.01	0.08689	0.09985	0.01701
24.01	0.07983	0.09523	0.01492
25.01	0.07363	0.0909	0.01322
26.01	0.06764	0.08651	0.01168
27.01	0.06217	0.0825	0.01027
28.01	0.05718	0.07844	0.009083
29.01	0.05272	0.07471	0.007966
30.01	0.04861	0.07102	0.007016
31.01	0.04458	0.06742	0.006182
32.01	0.04098	0.06404	0.005393
33.01	0.03794	0.06131	0.004762
34.01	0.03482	0.05836	0.00411
35.01	0.0319	0.05525	0.003671
36.01	0.02945	0.05269	0.003204
37.01	0.02723	0.05022	0.002901
38.01	0.02509	0.04788	0.002536
39.01	0.02288	0.04576	0.002207
39.99	0.02102	0.04357	0.001962

Table 3.1: Some values of $\mathcal{G}(p,\alpha,\mu)$ from the plots in figure 3.11.

3.4 Bare scheme update procedures for Σ^*

Rather than calculating $\mathcal{G}(\mathbf{p}, \tau)$ directly using DMC, it is also possible and even so preferred (motivate this from papers. Cover more diagrams and so on...) to instead simulate the proper self energy $\Sigma^*(\mathbf{p}, \tau)$, from which the electronic propagator is calculated using the Dyson equation (2.64). In order to do this, the random walk must now cover diagrams without external legs but also be able to reach the bare propagator $\mathcal{G}_0$ for normalization purposes. This is easily accomplished by a slight modification of some of the update procedures introduced in the previous section, and will be discussed in more detail shortly.

Before that however, it is important to realize that no longer all types of diagrams ($n > 0$) should be binned. In order to calculate Σ^* it is critical that the histogram N merely have contributions from irreducible diagrams. Then, in similarity to (3.21) and (3.22) the value of Σ^* is calculated in terms N_0 and N in the following way

$$\Sigma^*(\mathbf{p}_i, \tau_j) = N_{i,j} \frac{\sum_{k,l} \mathcal{G}_0(\mathbf{p}_k, \tau_l)}{N_0}, \quad \Sigma^*(\mathbf{p}_0, \tau_j) = N_j \frac{\sum_l \mathcal{G}_0(\mathbf{p}_0, \tau_l)}{N_0}. \tag{3.42}$$

An easy way to check whether or not a diagram is irreducible, is to store the current momentum of every $\mathcal{G}_0$ present in the diagram within a hash table. If one or more momenta are found to be equal to that of the external momentum, the diagram must clearly be reducible and should thus not be binned. Since the complexity of a search in a hash table is $\mathcal{O}(1)$, this implementation should not limit the performance of the algorithm.

Now, returning to the update procedures, there are only two which need to be modified. The others stay the same but might have some trivial change of notation for quantities, such as $\langle \mathbf{p} \rangle_{0,2n} \to \langle \mathbf{p} \rangle_{0,2n-1}$ in the case of the *change of external momentum* procedure.

Change of diagram length in time, type 1

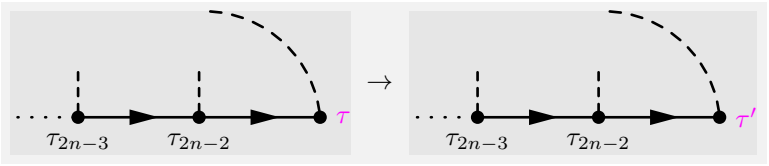

Figure 3.12: An illustration of the first kind of update procedure for changing the length of a diagram without external legs.

At $n > 0$, there is now a phonon propagator connected to the end point node of the diagram as depicted in figure 3.12. Thus, in accordance with the *change of diagram length in time, type 2* update procedure,

$$\frac{D_n(\tau')}{D_n(\tau)} = \exp\left\{-\left[\frac{p^2}{2} - \mu + 1\right](\tau' - \tau)\right\} . \tag{3.43}$$

Hence, to maintain the acceptance ratio at unity, the only modification needed is to change the rate parameter of the distribution from which τ' is sampled, i.e. $\lambda \to \lambda' = \lambda + 1$.

Change of diagram order

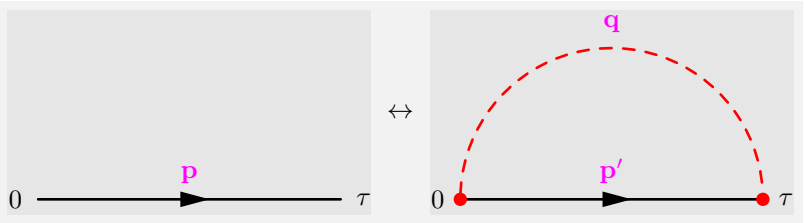

Figure 3.13: An illustration of the change of diagram order procedure between zeroth and first order diagrams.

In order to prevent generating diagrams with external legs, it is necessary only to modify the transition between a zeroth and a first order diagram. Instead of sampling two times where new nodes then will be inserted for the phonon to connect to, the already existing start and end point node of diagram will be used. This is illustrated in figure 3.13. Other than that this transition is no different from the ordinary *change of diagram order* update procedure so that

$$W(n = 0|n = 1) = P_{\mathrm{R}} \frac{\sin\theta_k}{2} \frac{1}{2\pi} \sqrt{\frac{2\tau}{\pi}} \exp\left\{-\frac{q_k^2}{2}\tau\right\} . \tag{3.44}$$

The acceptance ratio may thus be expressed as previously (3.40) with

$$\begin{aligned} R(n = 0|n = 1) &= \frac{D_{n=1}}{D_{n=0}} \frac{W(n = 1|n = 0)}{W(n = 0|n = 1)} \\ &= \frac{1 - P_{\mathrm{R}}}{P_{\mathrm{R}}} \frac{\alpha}{\sqrt{\pi}} \frac{1}{\sqrt{\tau}} \exp\left\{[\langle \mathbf{p} \rangle_{l,m-1} \cdot \mathbf{q}_k - 1]\tau\right\} . \end{aligned} \tag{3.45}$$

The transitions procedure between diagrams of order $n > 0$, as introduce in section 3.3, can not add any external legs since both the start and end point node

of the diagram will be connected to phonons. However, there are now $2n-1$ rather than $2n+1$ number of $\mathcal{G}_0$'s to chose from when sampling the starting point time of the phonon propagator. Hence the "$2n+1$" in equation (3.37) and (3.39) should be replaced by "$2n-1$" to incorporate this.

3.4.1 Divergent diagram

It can be shown that the first order self energy diagram $\Sigma^{*(1)}(\mathbf{p}, |tau)$ is proportional to $1/\sqrt{\tau}$ and thus diverges when $\tau \to 0$. It is not possible to capture such a behavior using a histogram since the function to be approximated has a too large second derivative in the vicinity of the singularity. To show this, consider the mean value of a function $f(x)$ on the interval $x_i - \Delta x/2 < x < x_i + \Delta x/2$ with $f(x_i)$ expanded in terms of the small parameter Δx, i.e.

$$\begin{aligned}
&\frac{1}{\Delta x}\int_{x_i-\Delta x/2}^{x_i+\Delta x/2} f(t)\,\mathrm{d}t \\
&\quad= \frac{1}{\Delta x}\int_{x_i-\Delta x/2}^{x_i+\Delta x/2} f(x_i+[t-x_i])\,\mathrm{d}t \\
&\quad= \frac{1}{\Delta x}\int_{x_i-\Delta x/2}^{x_i+\Delta x/2} \left[f(x_i)+f'(x_i)\,[t-x_i]+\tfrac{1}{2}f''(x_i)\,[t-x_i]^2+\cdots\right]\mathrm{d}t \\
&\quad= f(x_i)+\tfrac{1}{24}f''(x_i)\,[\Delta x]^2+\mathcal{O}([\Delta x]^4)\,.
\end{aligned} \tag{3.46}$$

In order for this mean value to be well approximated by $f(x_i)$, it is required that $f''(x_i)\,[\Delta x]^2 \ll f(x_i)$. However, in the case of $f(x) = 1/\sqrt{x}$ and $x_i = \Delta x/2$ this is not fulfilled, no matter the size of Δx, since $f''(x_i)\,[\Delta x]^2 = 3\sqrt{2}/\sqrt{\Delta x}$ whilst $f(x_i) = 2/\sqrt{\Delta x}$. The ability of a histogram to approximate the function $1/\sqrt{x}$ in the vicinity of $x = 0$ is illustrated in figure 3.14.

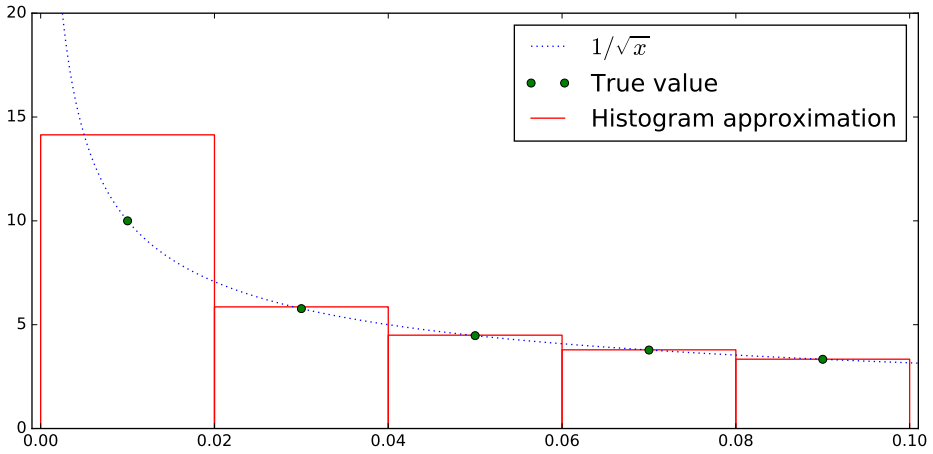

Figure 3.14: The function $1/\sqrt{x}$ approximated by a histogram with bin size $\Delta x = 0.02$ in the vicinity of $x = 0$. As can be seen, the approximative value at $x_0 = 0.01$ is quite far off from the true one.

The true value of the first order self energy diagram at zero external momentum is

$$\Sigma^{*(1)}(\mathbf{p} = \mathbf{0}, \tau) = \frac{\alpha}{\sqrt{\pi}} \frac{e^{-(1-\mu)\tau}}{\sqrt{\tau}} \quad \tau \geq 0\,. \tag{3.47}$$

When approximating this function with a histogram of bin size $\Delta\tau$, the value of the bin corresponding to τ_i becomes

$$\begin{aligned} &\langle \Sigma^{*(1)}(\mathbf{p} = \mathbf{0}) \rangle_j \\ &\quad = \frac{1}{\Delta\tau} \int_{\tau_j - \Delta\tau/2}^{\tau_j + \Delta\tau/2} \Sigma^{*(1)}(\mathbf{p} = \mathbf{0}, t)\, \mathrm{d}t \\ &\quad = \frac{1}{\Delta\tau} \frac{\alpha}{\sqrt{1-\mu}} \left[\mathrm{erf}\left\{ \sqrt{(1-\mu)\left(\tau_j + \tfrac{\Delta\tau}{2}\right)} \right\} - \mathrm{erf}\left\{ \sqrt{(1-\mu)\left(\tau_j - \tfrac{\Delta\tau}{2}\right)} \right\} \right] \end{aligned} \tag{3.48}$$

However, for external momentum $\mathbf{p} \neq \mathbf{0}$ it seems next to impossible to find an analytical expression of $\Sigma^{*(1)}(\mathbf{p}, \tau)$ due to cumbersome integrals. Nevertheless, by the usage of Monte Carlo integration these integrals may be calculated to an extremely good precision in a matter of seconds.

In order to find out whether a value of $\Sigma^{*(1)}(\mathbf{p}_i, \tau_j)$ should be calculated using DMC or Monte Carlo integration, it is reasonable to look at the difference $\Delta\Sigma_j^{*(1)} = \langle \Sigma^{*(1)}(\mathbf{p} = \mathbf{0}) \rangle_j - \Sigma^{*(1)}(\mathbf{p} = \mathbf{0}, \tau_j)$. For times $\tau_j < \tau_{\text{threshold}}$ where this difference is larger than a threshold value ε, Monte Carlo integration should be used, otherwise

DMC will be sufficient. The DMC code written during this master project has the threshold set to $\varepsilon = 0.001$. In table 3.2 the value of $\Delta\Sigma_j^{*(1)}$ is given for the first six j's.

j	0	1	2	3	4	5	6
$\Delta\Sigma_j^{*(1)}$	2.34	0.0486	0.0133	0.0058	0.00314	0.00193	0.00129

Table 3.2: Here $\Delta\Sigma_j^{*(1)}$ is calculated for different values of j. The parameters used are $\alpha = 1$, $\mu = -1.1$ and $\Delta\tau = 0.02$.

It is crucial that there will be no contribution from $\Sigma^{*(1)}$ to the histogram N for times where it is calculated using Monte Carlo integration. However, to avoid such a double contribution it is as simple as to not bin a first order self energy diagram if the length τ of which belongs to a bin $N_{i,j}$ of time $\tau_j < \tau_{\text{threshold}}$.

3.4.2 Results

Here follow some results obtained when simulating Σ^* using the bare scheme update procedures described above. For the same reasons as given before the external momentum $\mathbf{p}$ has again been kept fixed during these simulations .

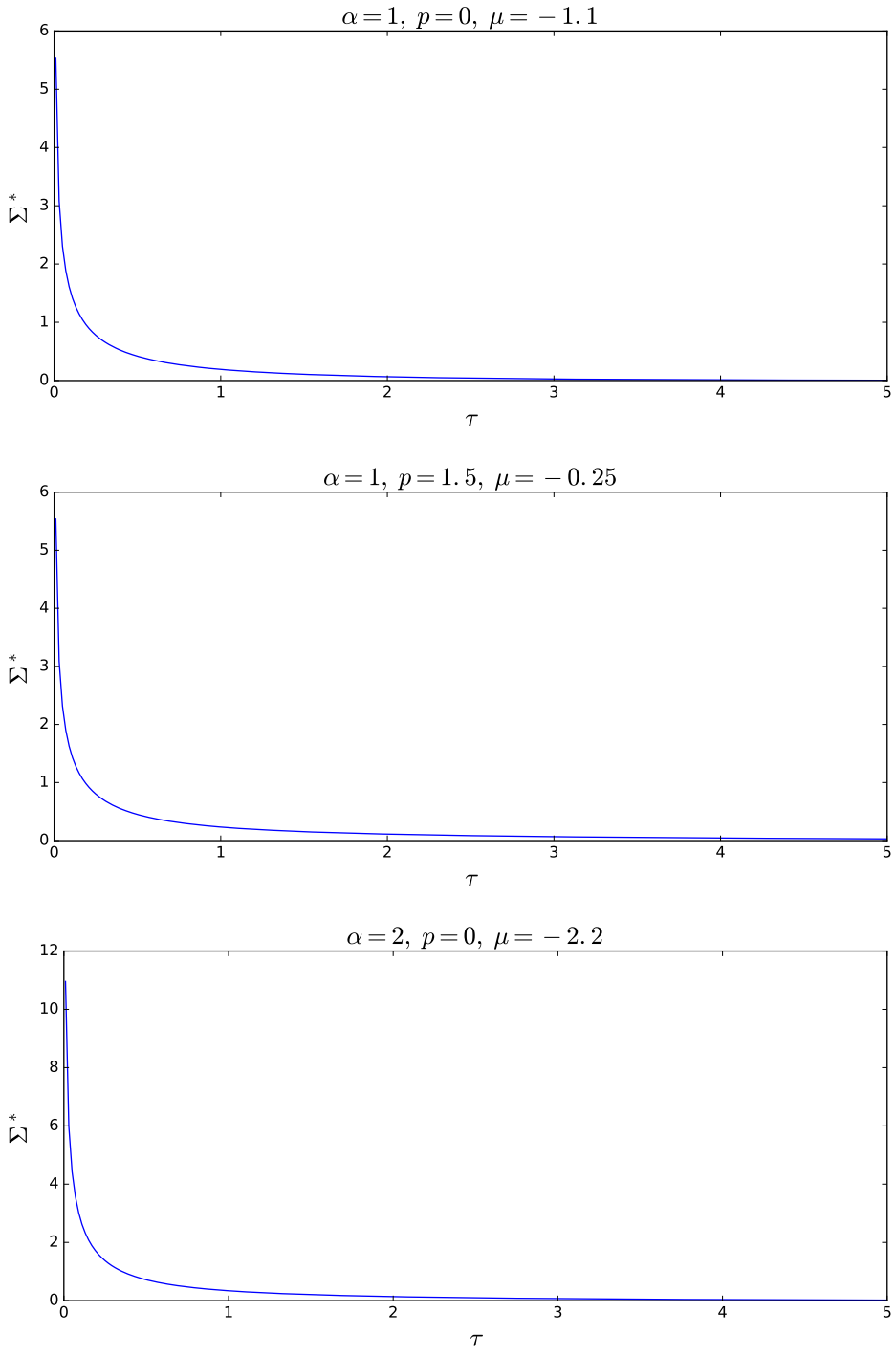

Figure 3.15: The acquired value of $\Sigma^*(p = 0,\ 0 \leq \tau \leq 5)$ after 80 minutes of core time. Here $\tau_{max} = 40$ and $\Delta\tau = 0.02$ has been used.

τ	$\Sigma^*(0,1,-1.1)$	$\Sigma^*(1.5,1,-0.25)$	$\Sigma^*(0,2,-2.2)$
0.01	5.531	5.537	10.96
0.21	0.892	0.9145	1.591
0.41	0.5063	0.5362	0.8721
0.61	0.3417	0.3757	0.5845
0.81	0.2484	0.2877	0.4318
1.01	0.1889	0.2312	0.3366
1.21	0.1481	0.1924	0.2724
1.41	0.1184	0.1638	0.2249
1.61	0.09575	0.1419	0.1887
1.81	0.07845	0.1248	0.1613
2.01	0.0643	0.1114	0.1377
2.21	0.05323	0.0994	0.1191
2.41	0.04421	0.08949	0.103
2.61	0.03667	0.08083	0.08986
2.81	0.03072	0.07354	0.07825
3.01	0.02576	0.06704	0.06804
3.21	0.02159	0.06117	0.05961
3.41	0.01814	0.05634	0.05227
3.61	0.01523	0.05141	0.046
3.81	0.01287	0.04739	0.04028
4.01	0.0109	0.04374	0.03547
4.21	0.009089	0.04027	0.03091
4.41	0.007704	0.03723	0.02729
4.61	0.006375	0.03454	0.02392
4.81	0.00551	0.03193	0.02108
4.99	0.004662	0.02981	0.01871

Table 3.3: Some values of $\Sigma^*(p,\alpha,\mu)$ from the plots in figure 3.15.

3.4.3 Implementing Dyson equation numerically

It is not entirely trivial how to implement Dyson equation when having to use a discrete Fourier transform. First of all, the proper self energy must be transformed into frequency space, but due to the singularity at $\tau = 0$ it is not preferable to transform this quantity directly. However, knowing the analytical expression of this singular contribution, it can then be subtracted from the self energy so that the discrete Fourier transform may be applied to the resulting regular expression. The singular part is then Fourier transformed analytically and once in ω-space it is added to the transformed regular expression. That is,

$$\Sigma^*(\mathbf{p}_i,\omega_j) = \mathcal{F}_{\mathrm{DFT}}\left\{\Sigma^*(\mathbf{p}_i,\tau_j) - \Sigma^*_{\mathrm{singular}}(\mathbf{p}_i,\tau_j)\right\} + \Sigma^*_{\mathrm{singular}}(\mathbf{p}_i,\omega_j)\,, \qquad (3.49)$$

which is possible due to the linearity of the Fourier transform. A possible choice of the singular part is $\Sigma^*_{\text{singular}}(\mathbf{p}_i, \tau_j) = \Sigma^{*(1)}(\mathbf{p} = \mathbf{0}, \tau_j)$ for which the expression is (3.47) and thus

$$\Sigma^*_{\text{singular}}(\mathbf{p}_i, \omega_j) = \frac{\alpha}{\sqrt{1 - \mu + i\omega_j}}\,. \tag{3.50}$$

Having the proper self energy in momentum and frequency space, Dyson equation is given by (2.64). However, it is not possible to directly transform back to $\mathcal{G}(\mathbf{p}_i, \tau_j)$ using the inverse discrete Fourier transform. This has to do with the fact that $\mathcal{G}(\mathbf{p}, \omega)$ falls of as $1/\omega$ when $\omega \to \infty$, which it too slow. Instead one may transform the difference

$$\Delta\mathcal{G}(\mathbf{p}, \omega) = \mathcal{G}(\mathbf{p}, \omega) - \mathcal{G}_0(\mathbf{p}, \omega) = \frac{\Sigma^*(\mathbf{p}, \omega)}{(i\omega + \xi(\mathbf{p}) - \Sigma^*(\mathbf{p}, \omega))\,(i\omega + \xi(\mathbf{p}))} \tag{3.51}$$

which has the proportionality $\Delta\mathcal{G}(\mathbf{p}, \omega \to \infty) \propto \omega^{-5/2}$ because $\Sigma^*(\mathbf{p}, \omega \to \infty) \propto \omega^{-1/2}$. Since also the inverse Fourier transform is linear, it follows that

$$\mathcal{F}^{-1}_{DFT}\left\{\Delta\mathcal{G}(\mathbf{p}_i, \omega_j)\right\} = \Delta\mathcal{G}(\mathbf{p}_i, \tau_j) = \mathcal{G}(\mathbf{p}_i, \tau_j) - \mathcal{G}_0(\mathbf{p}_i, \tau_j)\,. \tag{3.52}$$

The interacting electronic propagator in τ-space is finally obtained by

$$\mathcal{G}(\mathbf{p}_i, \tau_j) = \mathcal{G}_0(\mathbf{p}_i, \tau_j) + \Delta\mathcal{G}(\mathbf{p}_i, \tau_j)\,. \tag{3.53}$$

In figure 3.16 the relative difference between the $\mathcal{G}_{\Sigma^*}$ obtained using Dyson equation and the directly simulated $\mathcal{G}$ is plotted against τ for both $\Delta\tau = 0.02$ and $\Delta\tau = 0.01$. As can be seen the difference is smaller than the size of $\Delta\tau$ in both cases. The agreement also seems to improve somewhat linearly with smaller $\Delta\tau$, the drawback is however more noise since there is less statistics contributing to each bin N_j.

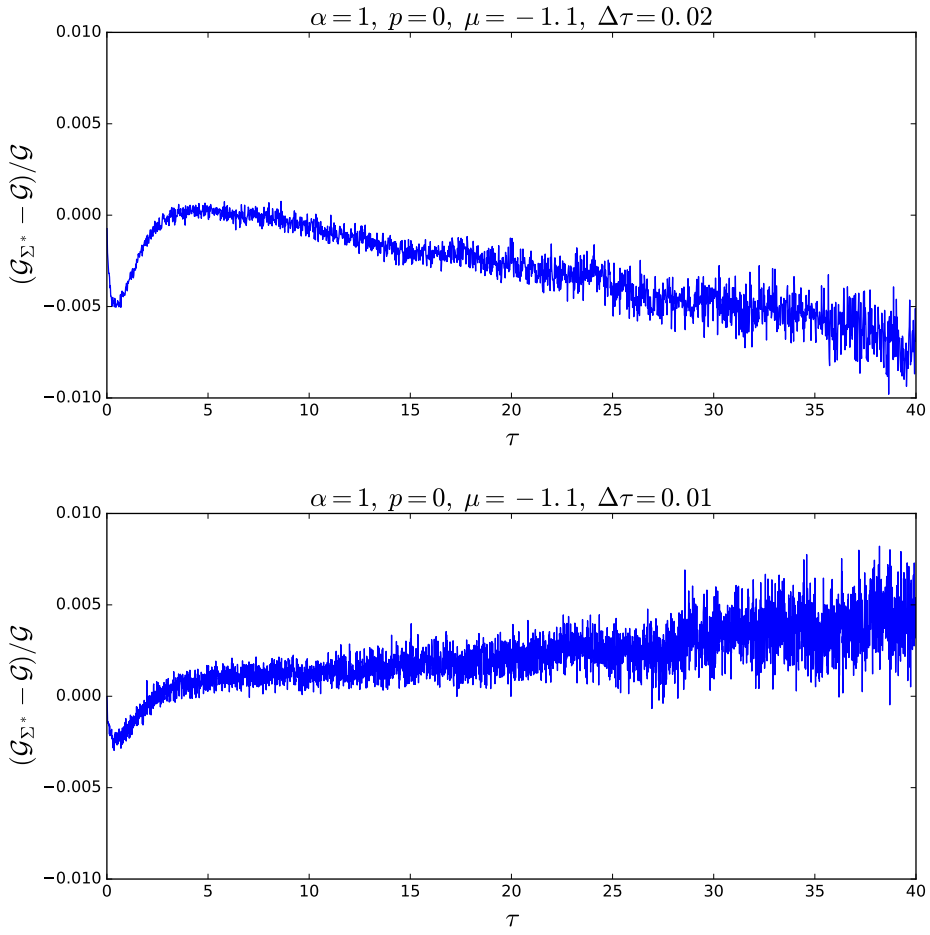

Figure 3.16: The relative difference between $\mathcal{G}_{\Sigma^*}$ obtained using Dyson equation and the directly simulated $\mathcal{G}$. For each of these simulations a core time of 24 hours has been used.

3.5 Bold-line scheme ?

The bold-line scheme [5] is a self consistent scheme making use of bold-line tricks iteratively in order to partially of fully sum up a diagram series. Dyson equation is one such bold-line trick and is the only one to be investigated in this thesis.

Here the propagator $\mathcal{G}_{i+1} = \mathcal{G}^{(0)} + \Delta\mathcal{G}_{i+1}$ is obtained when employing Dyson equation to the self energy S_{i+1}, made up of self energy diagrams subjected to certain constraints in order to prevent double counting. However, rather than using

the bare propagator when calculating S_{i+1}, the $\mathcal{G}_i$ computed in the previous iteration of the scheme is instead used. During the first iteration, when no propagator previously have been calculated, the bare one is used, i.e. $\mathcal{G}_0 = \mathcal{G}^{(0)}$. This scheme will converge given an appropriate choice of parameters so that $S_{m+1} \simeq S_m$ for some m. In practice, as will be shown, this convergence will happen after 4 or so iterations.

3.5.1 Skeleton diagrams

In order for certain diagrams to not contribute more than once to $\mathcal{G}_i$, it is necessary to narrow down the class of allowed diagrams to a subclass of the proper self energy diagrams referred to as skeleton diagrams [6]. This diagram class is characterized by the lack of insertions, i.e. diagram parts which act like self energies to some of the constituents of the diagram. This is illustrated in figure 3.17 with diagrams present in the series of $\mathcal{G}$.

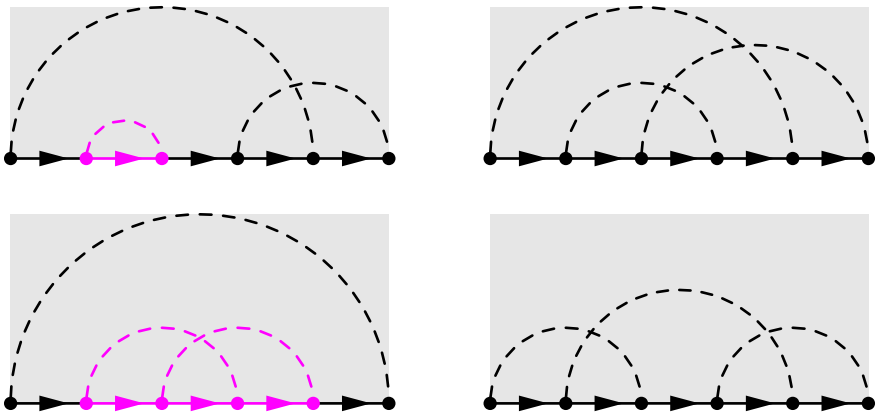

Figure 3.17: caption me please

- By putting an upper bound $n \leq n_{\max}$ of the generated diagrams in the Markov process...

To illustrate...

For simplicity it is used that $n_{\max} = 1$ so that

First iteration

$\Sigma_1^* =$ 

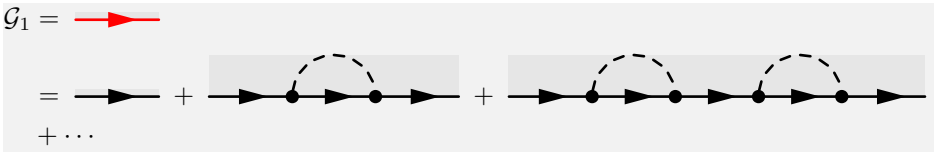

(3.54)

Second iteration

During the simulation of Σ_2^*, the propagator $\mathcal{G}_1$, obtained from the first iteration, is used in favor of the bare $\mathcal{G}^{(0)}$. Hence

and according to dyson Dyson equation

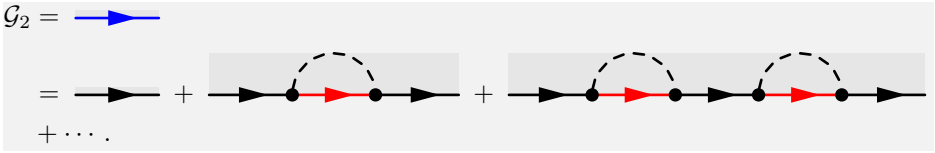

By substituting with the diagram series for $\mathcal{G}_1$ (3.54), $\mathcal{G}_2$ is expressed entirely out of bare constituents, i.e.

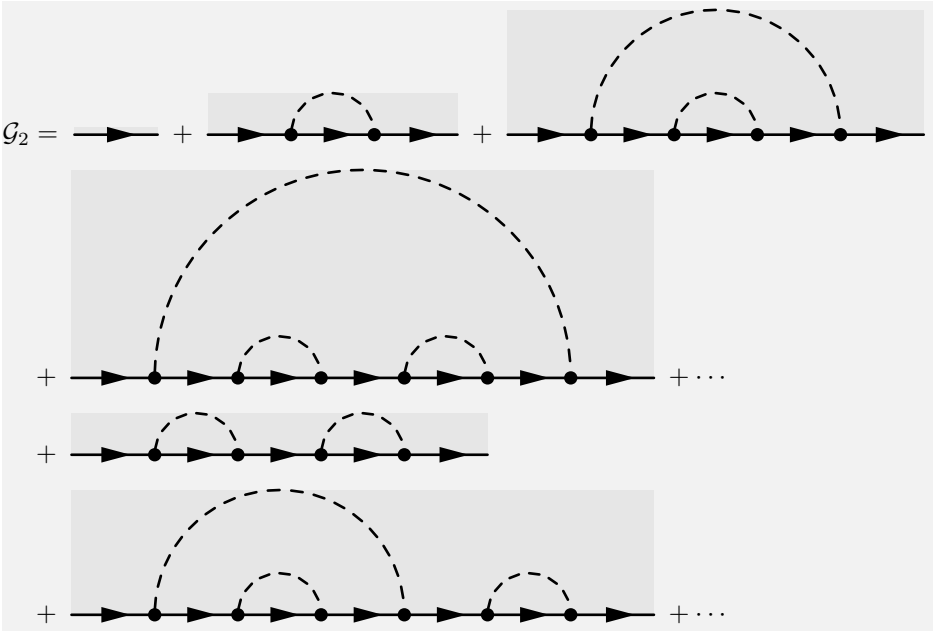

- Diagram with intersecting phonon lines wont appear in this diagram series...

3.5.2 Update procedures

3.5.3 Results

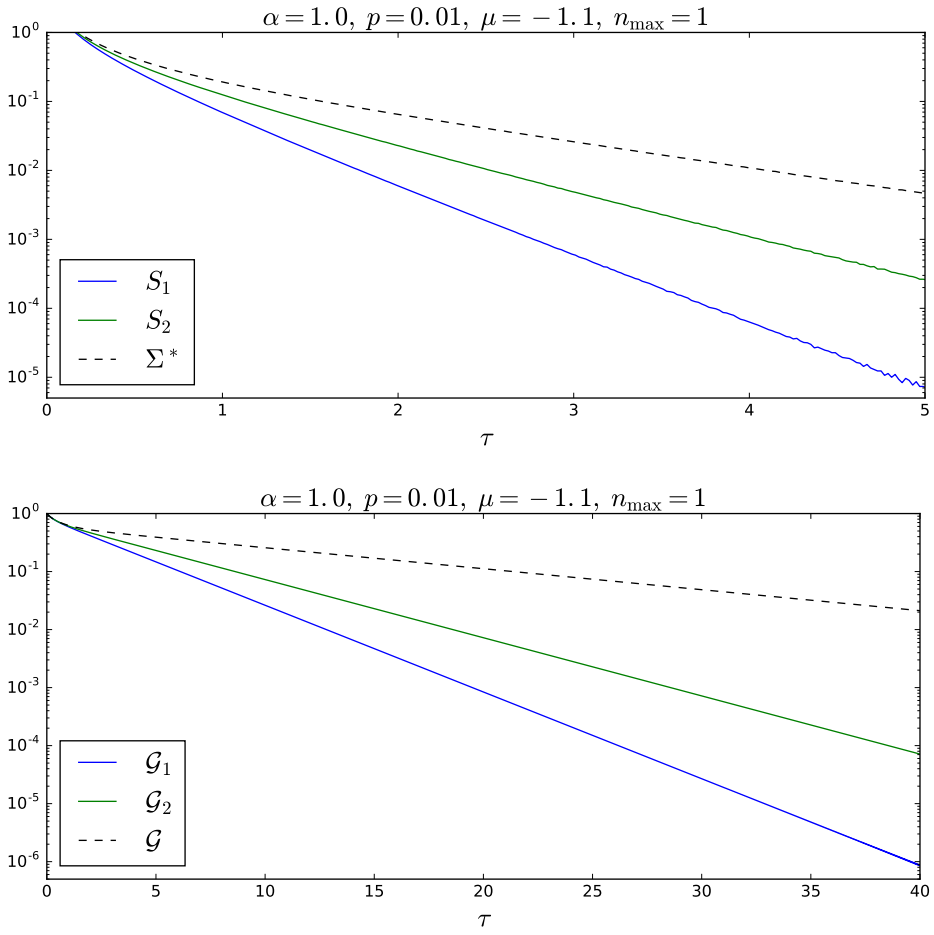

Figure 3.18: caption me plx

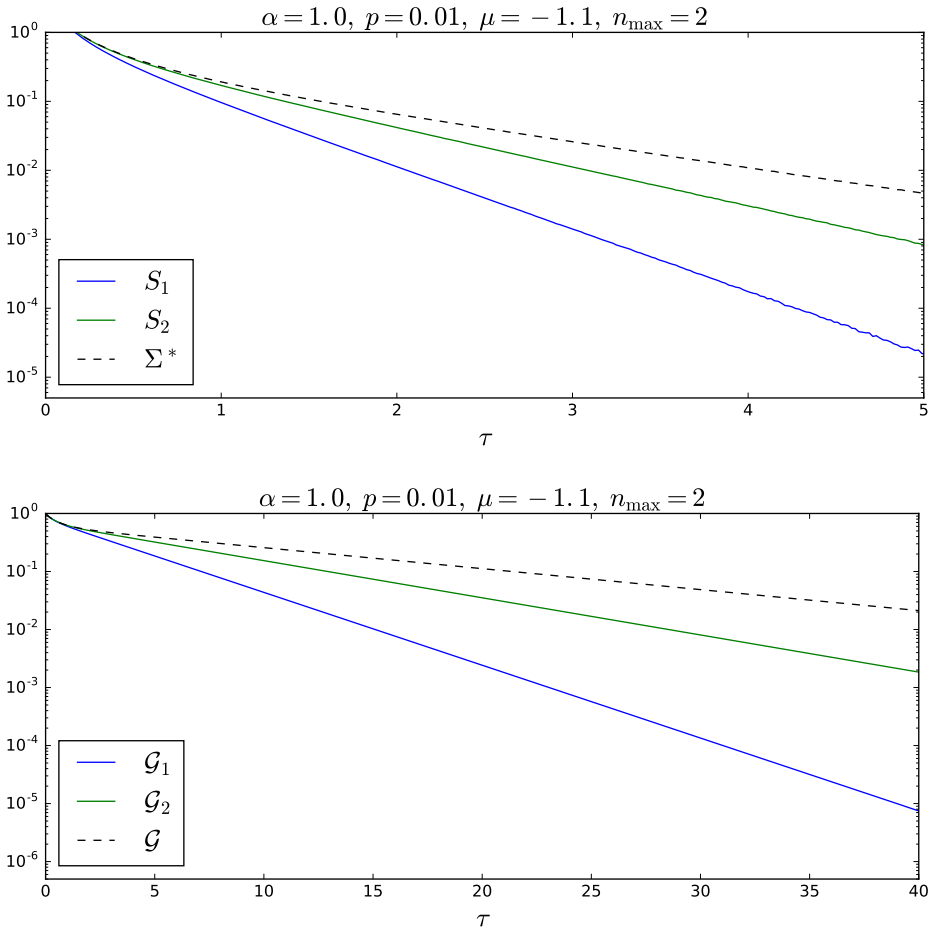

Figure 3.19: caption me plx

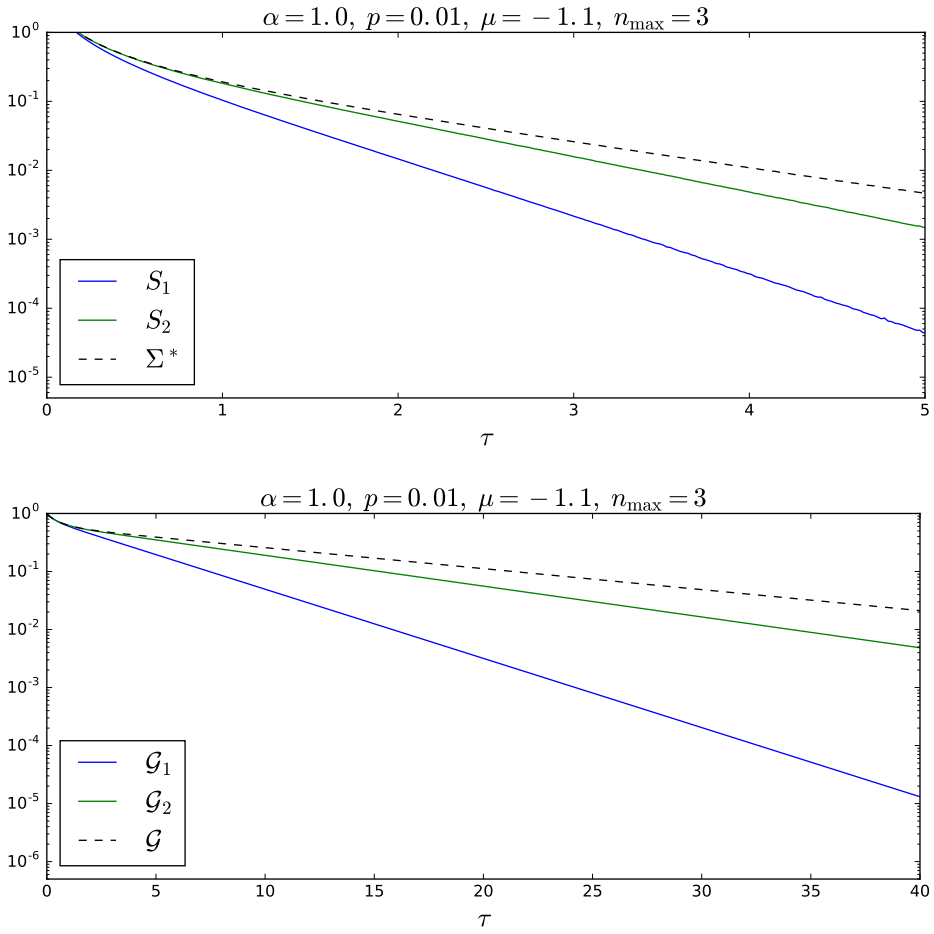

Figure 3.20: caption me plx

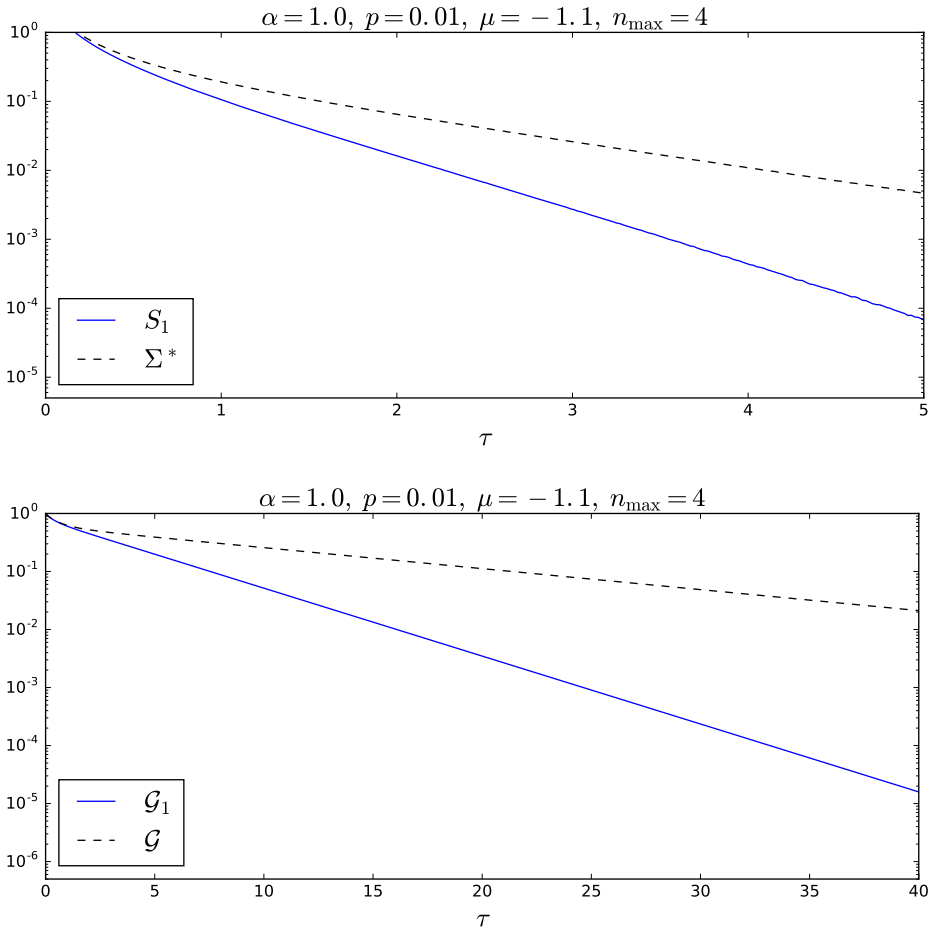

Figure 3.21: caption me plx

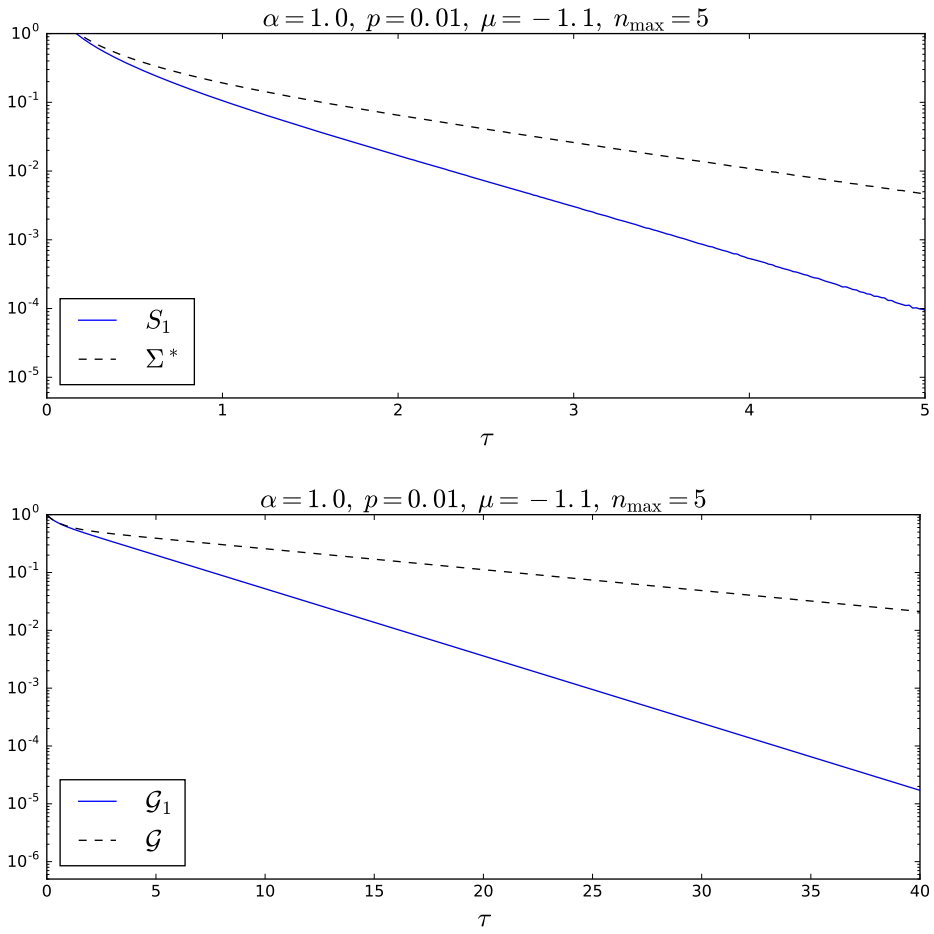

Figure 3.22: caption me plx

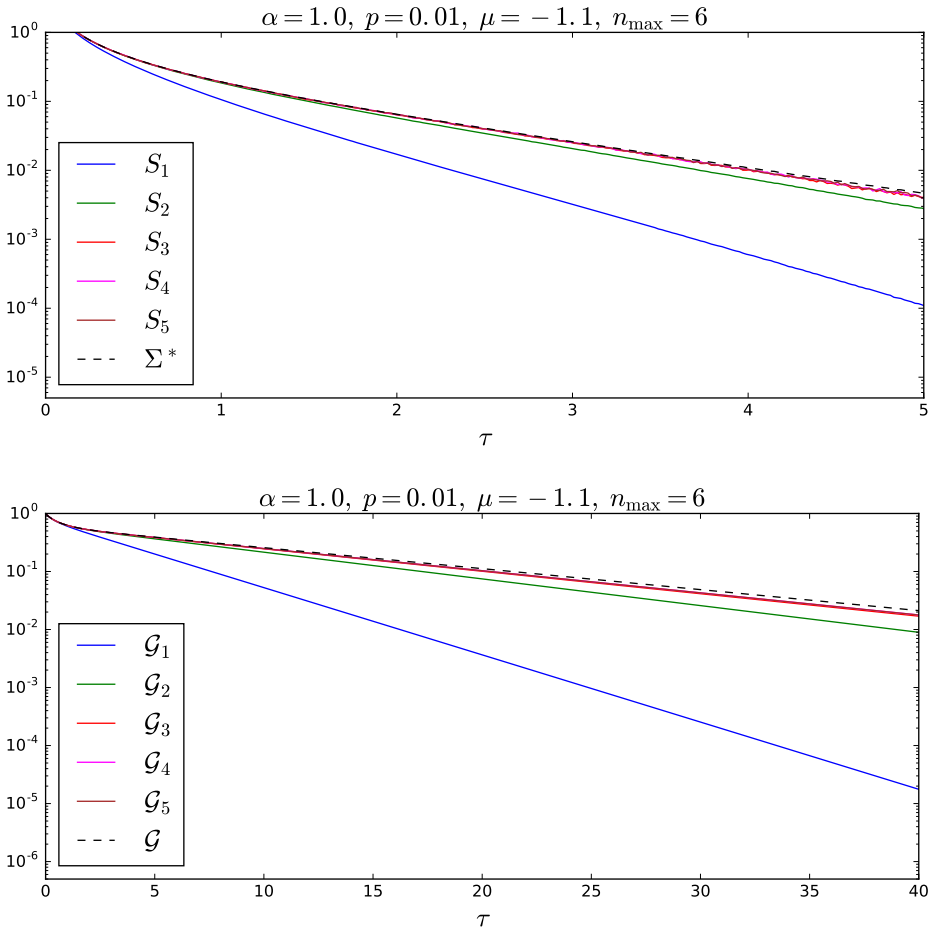

Figure 3.23: caption me plx

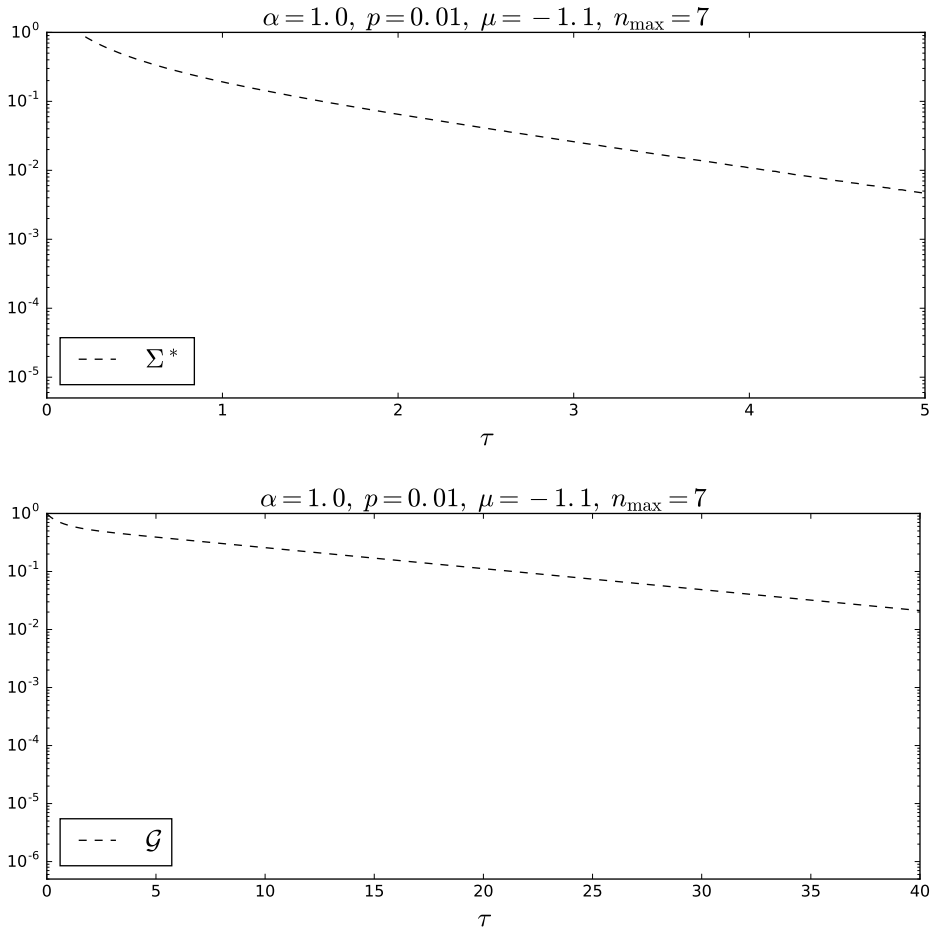

Figure 3.24: caption me plx

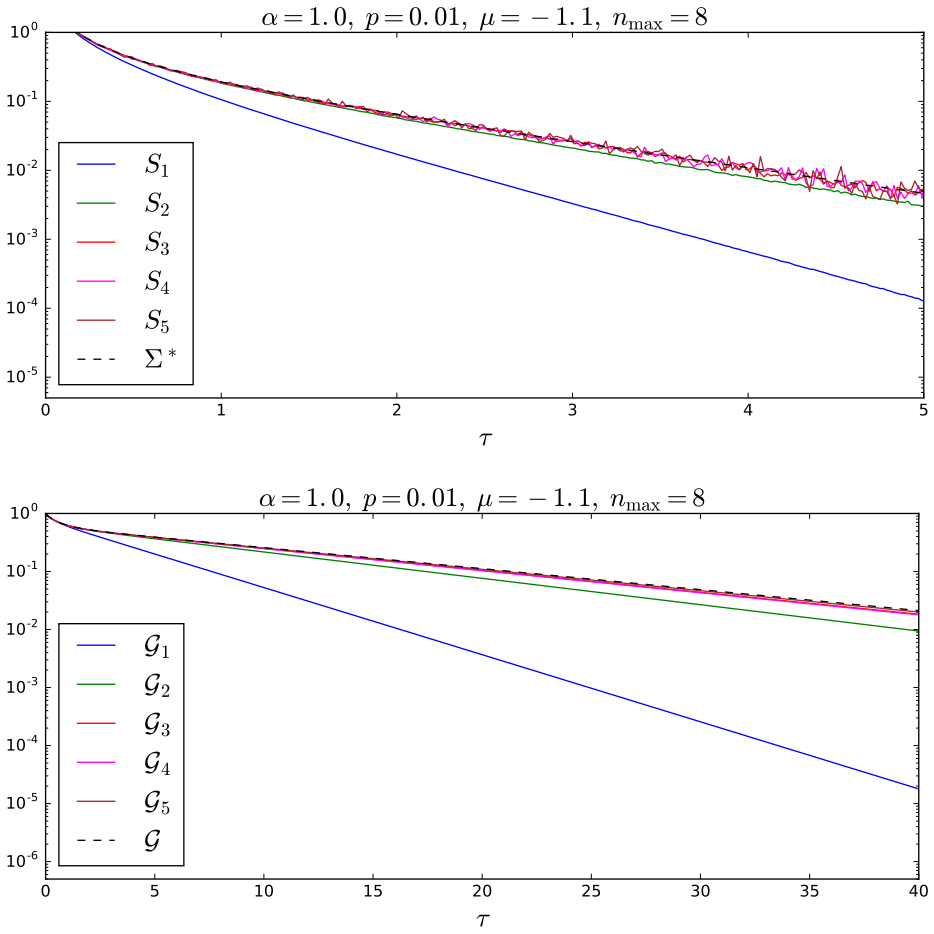

Figure 3.25: caption me plx

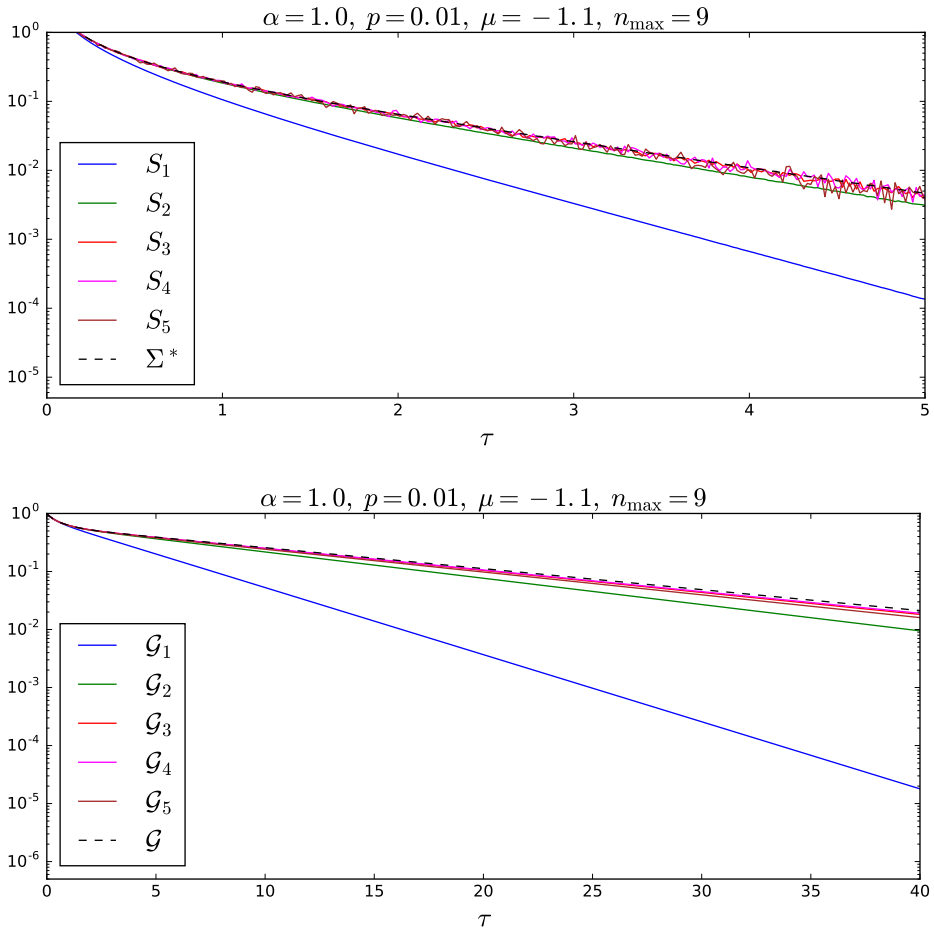

Figure 3.26: caption me plx

- E vs #iteration plot

3.6 Numerical Results

Chapter 4

Summary and Conclusions

Here we shall summarise what this chapter is about

Bibliography

[1] A. L. Fetter and J. D. Walecka, *Quantum Theory of Many-Particle Systems* (Dover Publications, 2003).

[2] A. Mishchenko *et al.*, *Diagrammatic quantum Monte Carlo study of the FrÃ¶hlich polaron*, Physical Review B **62**, 6317 (2000).

[3] H. FrÃ¶hlich, *Electrons in lattice fields*, Advances in Physics **3**, 325 (1954), `http://dx.doi.org/10.1080/00018735400101213`.

[4] N. V. P. Boris V. Svistunov, Egor S. Babaev, *Superfluid States of Matter* (CRC Press, 2015).

[5] N. Prokof'ev and B. Svistunov, *Bold Diagrammatic Monte Carlo Technique: When the Sign Problem Is Welcome*, Phys. Rev. Lett. **99**, 250201 (2007).

[6] R. Mattuck, *A Guide to Feynman Diagrams in the Many-Body Problem: Second Edition*Dover Books on Physics (Dover Publications, 2012).